

**UNIVERSIDAD DE INVESTIGACIÓN DE
TECNOLOGÍA EXPERIMENTAL YACHAY**

Escuela de Ciencias Químicas e Ingeniería

**TÍTULO: Orbital coupling and the dependence of mechanical
deformation in molecular structures**

Trabajo de integración curricular presentado como requisito para
la obtención del título de Químico

Autor:

Andino Enríquez José Esteban

Tutores:

Solmar Varela Salazar, Ph.D.

Thibault Terencio, Ph.D.

Urcuquí, Marzo 2020

Urcuquí, 12 de marzo de 2020

SECRETARÍA GENERAL
 (Vicerrectorado Académico/Cancillería)
ESCUELA DE CIENCIAS QUÍMICAS E INGENIERÍA
CARRERA DE QUÍMICA
ACTA DE DEFENSA No. UITEY-CHE-2020-00011-AD

En la ciudad de San Miguel de Urcuquí, Provincia de Imbabura, a los 12 días del mes de marzo de 2020, a las 15:00 horas, en el Aula CHA-02 de la Universidad de Investigación de Tecnología Experimental Yachay y ante el Tribunal Calificador, integrado por los docentes:

Presidente Tribunal de Defensa Dra. LOPEZ GONZALEZ, FLORALBA AGGENY , Ph.D.
Miembro No Tutor Dr. CAETANO SOUSA MANUEL , Ph.D.
Tutor Dra. VARELA SALAZAR, SOLMAR ALEXANDRA , Ph.D.

Se presenta el(la) señor(ita) estudiante **ANDINO ENRIQUEZ, JOSE ESTEBAN**, con cédula de identidad No. **0503149593**, de la **ESCUELA DE CIENCIAS QUÍMICAS E INGENIERÍA**, de la Carrera de **QUÍMICA**, aprobada por el Consejo de Educación Superior (CES), mediante Resolución **RPC-SO-39-No.456-2014**, con el objeto de rendir la sustentación de su trabajo de titulación denominado: **Orbital coupling and the dependence of mechanical deformation in molecular structures**, previa a la obtención del título de **QUÍMICO/A**.

El citado trabajo de titulación, fue debidamente aprobado por el(los) docente(s):

Tutor Dra. VARELA SALAZAR, SOLMAR ALEXANDRA , Ph.D.
Co - Tutor Dr. THIBAUT TERENCIO , Ph.D.

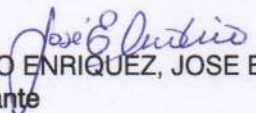
Y recibió las observaciones de los otros miembros del Tribunal Calificador, las mismas que han sido incorporadas por el(la) estudiante.

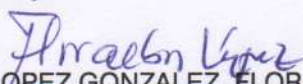
Previamente cumplidos los requisitos legales y reglamentarios, el trabajo de titulación fue sustentado por el(la) estudiante y examinado por los miembros del Tribunal Calificador. Escuchada la sustentación del trabajo de titulación, que integró la exposición de el(la) estudiante sobre el contenido de la misma y las preguntas formuladas por los miembros del Tribunal, se califica la sustentación del trabajo de titulación con las siguientes calificaciones:


Tipo	Docente	Calificación
Presidente Tribunal De Defensa	Dra. LOPEZ GONZALEZ, FLORALBA AGGENY , Ph.D.	10,0
Tutor	Dra. VARELA SALAZAR, SOLMAR ALEXANDRA , Ph.D.	10,0
Miembro Tribunal De Defensa	Dr. CAETANO SOUSA MANUEL , Ph.D.	10,0

Lo que da un promedio de: **10 (Diez punto Cero)**, sobre 10 (diez), equivalente a: **APROBADO**

Para constancia de lo actuado, firman los miembros del Tribunal Calificador, el/la estudiante y el/la secretario ad-hoc.


ANDINO ENRIQUEZ, JOSE ESTEBAN
 Estudiante


 Dra. LOPEZ GONZALEZ, FLORALBA AGGENY , Ph.D.
 Presidente Tribunal de Defensa


 Dra. VARELA SALAZAR, SOLMAR ALEXANDRA , Ph.D.
 Tutor



Dr. CAETANO SOUSA MANUEL, Ph.D.
Miembro No Tutor

ESCOBAR LANDAZURI, ANA MARIA
Secretario Ad-hoc

En la ciudad de San Miguel de Utcupuz, Provincia de Imbabura, a los 12 días del mes de marzo de 2020, en el Aula CHA-02 de la Universidad de Investigación de Tecnología Experimental Yachay y ante el Tribunal Calificador, integrado por los docentes:

Presidente Tribunal de Defensa: Dr. LÓPEZ GONZÁLEZ FLORALBA AGENY, Ph.D.
Miembro No Tutor: Dr. CAETANO SOUSA MANUEL, Ph.D.
Tutor: Dra. VARELA SALAZAR SOLIMAR ALEXANDRA, Ph.D.

Se presenta el(los) estudiante(s) ANDINO ENRIQUEZ JOSE ESTEBAN, con cédula de identidad No. 0803148883, de la ESCUELA DE CIENCIAS QUÍMICAS E INGENIERÍA, de la Carrera de QUÍMICA, aprobada por el Consejo de Educación Superior (CES), mediante Resolución RFO-08-14-005-2014, con el objeto de rendir la sustentación de su trabajo de titulación denominado: "Optical coupling and the development of mechanical deformation in molecular structures, previa a la obtención del título de QUÍMICO".

El(los) trabajo(s) de titulación, los debidamente aprobados por el(los) docente(s):

Tutor: Dra. VARELA SALAZAR SOLIMAR ALEXANDRA, Ph.D.
Co-Tutor: Dr. THIBAUT TERNON, Ph.D.

Y recibió las observaciones de los otros miembros del Tribunal Calificador, las mismas que han sido incorporadas por el(los) estudiante(s).

Previamente cumplidos los requisitos legales y reglamentarios, el trabajo de titulación fue sustentado por el(los) estudiante(s) examinado por los miembros del Tribunal Calificador. En su virtud la sustentación del trabajo de titulación, que integró la exposición de el(los) estudiante(s) sobre el contenido de la misma y las preguntas formuladas por los miembros del Tribunal, se califica la sustentación del trabajo de titulación con las siguientes calificaciones:

Nombre del Estudiante	Calificación
Presidente Tribunal De Defensa Dr. LÓPEZ GONZÁLEZ FLORALBA AGENY, Ph.D.	100
Tutor Dra. VARELA SALAZAR SOLIMAR ALEXANDRA, Ph.D.	100
Miembro Tribunal De Defensa Dr. CAETANO SOUSA MANUEL, Ph.D.	100

Lo que da un promedio de: 10 (Días punto Caro), sobre 10 (diez), equivalente a: APROBADO.

Para constancia de lo actuado, firman los miembros del Tribunal Calificador, el(los) estudiante(s) y el(los) secretario(s) ad-hoc:

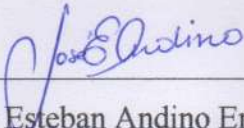


ANDINO ENRIQUEZ JOSE ESTEBAN
Dr. LÓPEZ GONZÁLEZ FLORALBA AGENY, Ph.D.
Presidente Tribunal de Defensa
Dra. VARELA SALAZAR SOLIMAR ALEXANDRA, Ph.D.
Tutor

AUTORÍA

Yo, **José Esteban Andino Enríquez**, con cédula de identidad 0503149593, declaro que las ideas, juicios, valoraciones, interpretaciones, consultas bibliográficas, definiciones y conceptualizaciones expuestas en el presente trabajo; así como, los procedimientos y herramientas utilizadas en la investigación, son de absoluta responsabilidad del autor del trabajo de integración curricular. Así mismo, me acojo a los reglamentos internos de la Universidad de Investigación de Tecnología Experimental Yachay.

Urcuquí, Marzo 2020.



Jose Esteban Andino Enríquez
CI: 0503149593

AUTORIZACIÓN DE PUBLICACIÓN

Yo, **JOSÉ ESTEBAN ANDINO ENRÍQUEZ**, con cédula de identidad 0503149593, cedo a la Universidad de Investigación de Tecnología Experimental Yachay, los derechos de publicación de la presente obra, sin que deba haber un reconocimiento económico por este concepto. Declaro además que el texto del presente trabajo de titulación no podrá ser cedido a ninguna empresa editorial para su publicación u otros fines, sin contar previamente con la autorización escrita de la Universidad.

Asimismo, autorizo a la Universidad que realice la digitalización y publicación de este trabajo de integración curricular en el repositorio virtual, de conformidad a lo dispuesto en el Art. 144 de la Ley Orgánica de Educación Superior

Urcuquí, Marzo y 2020.



JOSE ESTEBAN ANDINO ENRÍQUEZ
CI: 0503149593

Acknowledgements

A mis padres me enseñaron la vida.

A mis hermanos que enseñaron como vivir la vida.

A mis amigos con quienes he vivido esa vida.

A mis profesores que me han aconsejado, me han guiado y se han convertido en amigos.

A las madrugadas.

A los malos momentos.

A las caídas.

Gracias.

Abstract

Orbital coupling and the dependence of mechanical deformation in molecular structures

José Esteban Andino Enríquez

Yachay Tech University

Se han desarrollado varios modelos teóricos para comprender la relación entre la transmisión electrónica a través de moléculas orgánicas, la quiralidad de las estructuras y la orientación del spin del electrón, que explican la alta polarización del spin observada en resultados experimentales. Los modelos teóricos analíticos contemplan el Hamiltoniano asociado con el movimiento de un electrón a través de la molécula, incluyendo la contribución de las interacciones Spin-Orbit (SO) y el solapamiento de orbitales para los términos cinéticos.

En este trabajo, se realiza un modelo Tight-Binding que incluye elementos Slater-Koster para representar la contribución del solapamiento de orbitales en estructuras moleculares. Se incluye una dependencia explícita de las variables físicas que describen las moléculas (radio, pitch, la distancia entre átomos, entre otros) y una base orbital 2p en una estructura general para determinar expresiones generales de elementos Slater-Koster en un sistema de coordenadas específico. Estos elementos son una representación cuántica del enlace químico entre dos átomos en una molécula. Con la parametrización correcta de la estructura molecular, se probó el comportamiento de la magnitud de las superposiciones de los orbitales con deformaciones mecánicas. Las expresiones propuestas reproducen los resultados analíticos obtenidos previamente para ADN y nanotubos y pueden usarse para describir otras estructuras, como benceno, oligopéptidos, entre otros.

Finalmente, fueron escritas diferentes rutas que conectan p_z orbital en átomos a través de los términos Slater-Koster, incluidas las interacciones SO y el efecto Stark que se pueden usar para generar una lista de términos en un modelo de Hamiltoniano Tight-Binding.

Abstract

Orbital coupling and the dependence of mechanical deformation in molecular structures

José Esteban Andino Enríquez

Yachay Tech University

Several theoretical models have been developed to understand the relationship between the electron transmission through organic molecules, the chirality structures, and the electron spin orientation, that explain the high polarization of spin observed in the experiments. Analytical theoretical models contemplate the Hamiltonian associated with the movement of an electron through the molecule, including the contribution of Spin-Orbit (SO) interactions, and orbital overlaps for the kinetic terms.

In this work, an analytical tight-binding model that includes Slater-Koster elements is derived to represent the contribution of orbital overlap in molecular structures. We include an explicit dependence on the physical variables that describe the molecules (radius, pitch, the distance between atoms, among others.) and one 2p-orbital-base by the site in a general structure to determine general expressions of the Slater-Koster elements in specific coordinate systems. These elements are a quantum representation of the chemical bond between two atoms in a molecule. With the right parametrization of the molecular structure, we tested the behavior of the magnitude of the orbital overlaps with mechanical deformations. Our expressions reproduce the previously obtained analytical results for DNA and nanotubes and can be used to describe other structures, like benzene, oligopeptides, among others. Finally, we write paths that connect p_z orbital in atoms through the Slater-Koster terms, including SO interactions and Stark effect that can be used to generate a list of terms in a Hamiltonian tight-binding model.

CONTENTS

Contents	vi
List of Figures	vii
List of Tables	viii
Introduction	1
1 Theoretical frame	5
1.1 Helicene: Structural Features	5
1.2 Benzene as the basic structure of Helicene	7
1.3 Slater-Koster terms overlaps and chemical bonds.	9
1.4 Atomic interactions	11
1.4.1 Spin-Orbit interaction	11
1.4.2 Stark effect	15
1.5 Computational Methodology	15
2 Computational analysis of the molecular structure: Helicene	17

3	Analytical Slater-Koster elements	22
3.1	Slater-Koster (SK) elements in general coordinate systems	22
3.1.1	SK elements with $\{s, p_x, p_y\}$ in the xy -plane and p_z orthogonal.	22
3.1.2	SK elements with $\{s, p_x, p_y\}$ in the xy -plane and p_z with a component in the z -axis.	27
3.1.3	Verification of the Slater-Koster expressions	32
3.2	Use of the SK model with a molecule example: Benzene	37
3.2.1	Benzene parameterization	37
3.2.2	The SK elements and the dependence with deformations in the benzene model	38
3.3	Chapter conclusions	41
4	Paths that connect p_z orbitals through interactions and the Slater-Koster terms	42
4.1	Chapter conclusions	45
	Conclusions	46
	Bibliography	48

LIST OF FIGURES

1.1	Helicene Structures with its respective pitch.	6
1.2	Resonance of Benzene.	7
1.3	Molar heats of hydrogenation of cyclohexene, cyclohexadiene and benzene.	8
1.4	Energy diagram of the molecular orbital of Benzene.	8
1.5	Diagram of the Slater-Koster parameters that represent the different types of σ and π bonds.	10
1.6	Spin-orbit interaction scheme.	11
2.1	Input with Dispersion Correction.	18
2.2	Input with No Dispersion Correction.	18
2.3	Code to show p-orbitals.	19
2.4	6 Benzene Rings-Helicene with: a) correction dispersion and b) no correction dispersion.	19
3.1	Scheme showing two orbitals located in R_i and R_j positions, and the unit vectors that indicate the direction of the atomic orbitals.	23
3.2	The SK overlap E_{sx} as a function of β for different values of θ . To calculate the values of $V_{\mu\mu'}$ the used distance between atoms is $\mathbf{R} = 1.42 \text{ \AA}$.	25

3.3	The SK overlap E_{xx} as a function of β for different values of θ . To calculate the values of $V_{\mu\mu'}$ the used distance between atoms is $\mathbf{R} = 1.42\text{\AA}$, $K_{pp}^{\sigma} = -0.81$ and $K_{pp}^{\pi} = 3.24$.	26
3.4	The SK overlap E_{xy} as a function of β for different values of θ . To calculate the values of $V_{\mu\mu'}$ the used distance between atoms is $\mathbf{R} = 1.42\text{\AA}$, $K_{pp}^{\sigma} = -0.81$ and $K_{pp}^{\pi} = 3.24$.	26
3.5	General scheme of orbitals overlap in a specific coordinate system. In this case, the p_z orbital has a component in the z -axis.	27
3.6	The SK overlap E_{xx} as a function of β for different values of θ . To calculate the values of $V_{\mu\mu'}$ the used distance between atoms is $\mathbf{R} = 1.42\text{\AA}$, $K_{pp}^{\sigma} = -0.81$ and $K_{pp}^{\pi} = 3.24$.	30
3.7	The SK overlap E_{xy} as a function of β for different values of θ . To calculate the values of $V_{\mu\mu'}$ the used distance between atoms is $\mathbf{R} = 1.42\text{\AA}$, $K_{pp}^{\sigma} = -0.81$ and $K_{pp}^{\pi} = 3.24$.	30
3.8	The SK overlap E_{yy} as a function of β for different values of θ . To calculate the values of $V_{\mu\mu'}$ the used distance between atoms is $\mathbf{R} = 1.42\text{\AA}$, $K_{pp}^{\sigma} = -0.81$ and $K_{pp}^{\pi} = 3.24$.	31
3.9	The SK overlap E_{yx} as a function of β for different values of θ . To calculate the values of $V_{\mu\mu'}$ the used distance between atoms is $\mathbf{R} = 1.42\text{\AA}$, $K_{pp}^{\sigma} = -0.81$ and $K_{pp}^{\pi} = 3.24$.	31
3.10	DNA molecular structure model in a XY plane[20]. For the equations shown, we used just to the verification that $b = 0$.	33
3.11	The our general scheme and the Nanotube model scheme that show the orientations of the orbitals.	34
3.12	General and the DNA model schemes that show the orientations of the orbitals. In the DNA model, b is the pitch of the molecule and a is the radius of the helix.	35
3.13	Benzene carbons in the X-Y plane where $\Delta\phi$ is the angle between consecutive carbons and \mathbf{R}_n is the distance between two atoms.	38
3.14	Representation of benzene's two p_x -orbitals coupling.	39
3.15	Representation of benzene's p_x^i and p_y^j orbitals coupling.	39
3.16	Representation of benzene's two p_y orbitals coupling.	40

LIST OF TABLES

1.1	Spin-Orbit coupling values.	12
1.2	Expected Spin-Orbit values that connect the atomic orbitals.	14
2.1	Results-Structure 1. (Fig 1.1 (a))	20
2.2	Results-Structure 2. (Fig 1.1 (b))	20
3.1	Slater-Koster overlaps between orbitals on sites i and j .	24
3.2	General Overlapping Equations	29
4.1	First order's possible paths from p_z^i to p_z^j .	43
4.2	Second order's possible paths from p_z^i to p_z^j .	44

INTRODUCTION

The concept of spintronic involves the study of the electron's spins transport with the purpose of transfer information and to perform computations. The main structures considered for this purpose in the context of the spintronic are inorganic metals, oxides, and semiconductors due to the considerable spin-orbit energy-level splittings associated with the atoms that conform to these systems. However, several recent experiments have shown that organic molecules with chirality (DNA [1], oligopeptides [?], Helicene [?], among others) could be used for spintronic applications due to the unusually large electron spin polarization during the electron transport, an effect known as Chiral Induced Spin Selectivity Effect (CISS) [3].

The word *chiral* was coined by William Thomson (Lord Kelvin) in 1894 to denote objects that are not superimposable with its mirror image [4]. These mirror images of a chiral molecule are named enantiomers and could be right or left-handed. Chirality is extremely important in organic chemistry, in biochemistry, in inorganic chemistry, among others, where it gives rise to stereochemistry to stereospecific reactions. In the CISS effect, when the electron moves through a chiral-organic molecule, it experiences the electrostatic potential of the molecule, which is also chiral [3]. If the chiral molecule is in a specific turn (clockwise or counterclockwise) and the electron, due it has a dipole moment associated

with its spin that makes it rotate in one direction according to the speed of the particle, they are in parallel. Then there is a movement of electrons that have the determined spin value in that direction through the structure. In the experiments, more were up to 60 percent spin polarization has been found. This results allow to chiral molecules the possibility of being used in the spintronic applications, such as the production of devices with greater energy efficiency and reduced size [5], chiral recognition[6], etc., and their use would be of the great advantage because this molecules are easy to produce, have flexibility properties, biological compatibility and are low cost.

The relationship between chiral molecules and the polarization of electronic spins is not entirely clear [7, ?, 3]. The presence of light atoms (like carbons) and the absence of strong magnetic centers is not enough to understand the high spin polarization obtained in the experiments, which is why a series of theoretical models have been proposed to explain the mechanism behind these results. Several theoretical models [5, 8, ?] have been proposed to describe the spin-orbit interactions which are decisive in explaining the spin selectivity in ring-shaped molecular structure. Varela and CO in their work [5] obtained an effective Hamiltonian for a helical structure-like DNA considering the explicit interaction between bases, including Slater-Koster (SK) elements for the overlap between orbitals and SO interaction. The effective interactions are represented in terms of paths connecting the orbitals with the SK elements and with Stark and Spin-Orbit (SO) interactions, at first order. The existence or not of a specific path is directly connected with the presence or not of these elements. At the same time, the presence of the SK elements depends on the parameters that describe the structure of the molecule (orientation, distances between atoms, etc.). The interaction could be tuned mechanically, changing the molecular structure [9, 10].

In general, computational chemical and analytical quantum methods would allow to evaluate the electron transport and bring a more detailed and adequate explanation about the orbital coupling and of the interactions present on organic molecules, to reach a theoretical interpretation about its spin selectivity transportation.

Based on previous justifications, the study of the atomic-orbital coupling using a Slater-Koster-type description in explicit function of the physical parameters of the molecular structure, and the analysis of the influence on the change of these parameters by deformations in the presence of the interactions was proposed as general objective. The specific objectives include:

1. To analyze using the computational method the distance of different Helicenes with L and D turn to test if the helical pitch changes.
2. To determine general expressions of the Slater-Koster elements with explicit dependence on the physical variables that describe the position of the atoms in a molecule, in a specific 2D coordinate system.
3. To analyze the behavior of the SK elements under the change of the physical parameters that describe the structure.
4. To use the general expressions obtained to derive the Slater-Koster elements from DNA and graphene, and compare with the literature.
5. To determine the Slater-Koster elements for the basic structure that makes up the Helicene (benzene) and study his behavior with changing parameters.
6. To analyze how molecular deformation and the presence of specific interactions (Spin-Orbit and Stark) influence the paths connected by the terms SK.

The content of this titling project is structured as follow:

The Chapter **1** deals with the structural features of Benzene as the basic structure of Helicene, the chemical bonds and Slater-Koster terms relationship, the description of the Spin-Orbit interaction, Stark effect, and the computational methodology. In the Chapter 2 is evaluated the computational analysis of molecular structure of Helicene where are

detailed the basis-set and method used for the analysis. Meanwhile, in the Chapter 3, are build analytical Slater-Koster elements for coordinate systems to model general equations to show the orbital overlapping process. The last chapter handles the feasible paths electrons can take in the electron transportation when Slater Koster elements, SO, and Stark coupling are presented. Finally, the Conclusions are presented.

1.1 Helicene: Structural Features.

Helicene is a polycyclic aromatic compound with nonplanar screw-shaped skeletons formed by ortho-fused benzene or other aromatic rings [11]. Due to the steric hindrance of its terminal rings, helicenes can wind itself in opposite directions and have a C_2 -symmetry [12]. This fact gives them chiral activity even though they do not have a chiral center and forming a pair of enantiomers P and M. If the helix rotates around the clockwise along the helical axis it is denoted as the enantiomer P. On the other hand, the one that turns counterclockwise is the enantiomer M [12].

As the benzene rings have resonance, Helicene can have two structures, as shown in Figure 1.1:

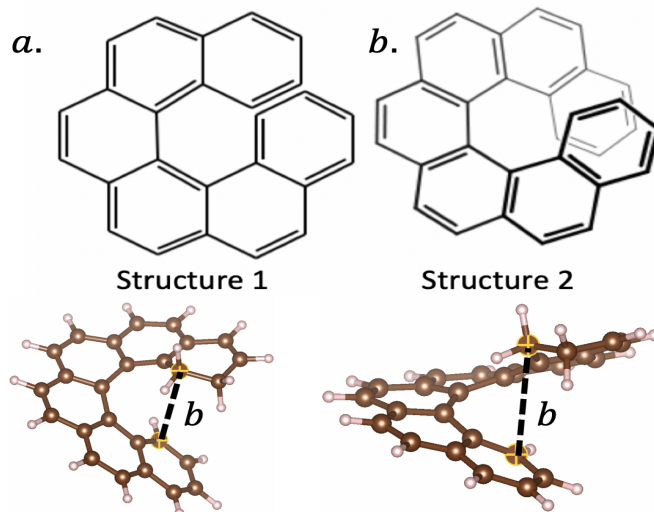


Figure 1.1: Helicene Structures with its respective pitch.

When Helicene has completed a 360° turn around the helical axis (usually completed with six benzene rings), the distance between the first benzene ring and the sixth ring in the chain is known as the helical pitch denoted by b (see Figure 1.1). As a member of the PAHs, Helicene is an excellent electron donor, and this makes an intriguing effect intrinsically present in the spin selectivity of the electron appears. Electrons have two properties: They have a negative charge and the spin. The spin is the intrinsic angular momentum of the electron and makes that it rotates clockwise or counterclockwise [3].

As a first approximation to describe Helicene, the structure is broken down in its fundamental units, that is to say, Benzenes and, in this way, all the possible overlaps between two atoms that are first neighbors in this structure are found. Then, by superposition, it can be extrapolated to a general behavior of Helicene.

1.2 Benzene as the basic structure of Helicene

In 1825, Faraday isolated a compound from illuminating gas with an empirical formula of CH . Then, Mitscherlich was able to measure its molecule mass, setting it to 78 *amu* (atomic mass units), obtaining the molecule formula C_6H_6 . Since the Mitscherlich obtained the compound from gum benzoin, he named it *Benzin*, now called *Benzene* [13].

Benzene is an aromatic hydrocarbon represented by a six-member ring with three conjugated double bonds with molecular formula C_6H_6 . The representation of the three double bonds is due to Kekulé. [13] Through his hypothesis, it was possible to arrive at the explanation of the resonance presented by benzene, where it was pointed out that in the structure, the single bond should be longer than the double bond. [13]

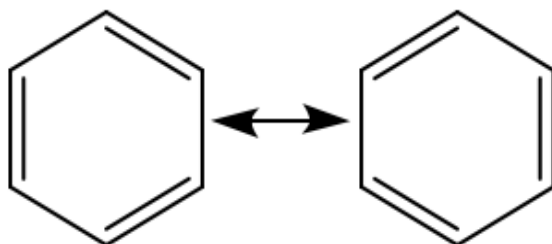


Figure 1.2: Resonance of Benzene.

The unexpected stability of benzene is attributed to the weak reactivity of benzene to substitutions compared to cyclohexadiene and cyclohexene. [13]

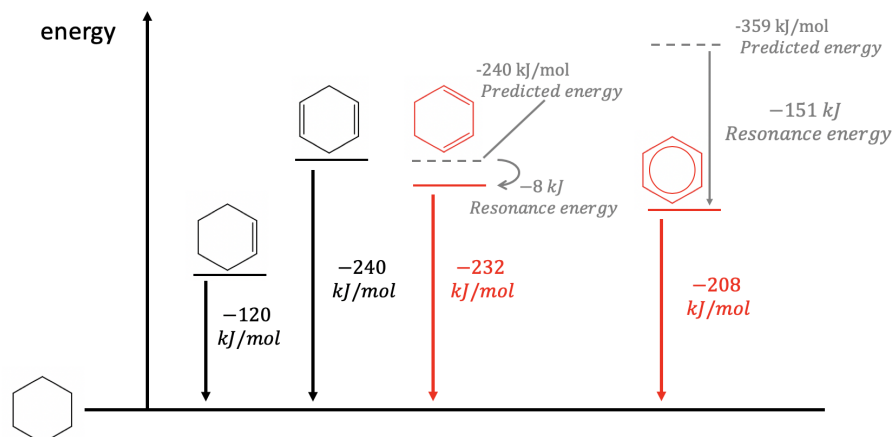


Figure 1.3: Molar heats of hydrogenation of cyclohexene, cyclohexadiene and benzene.

Figure 1.3 shows the molecular heats of hydrogenation of six-carbon ring-shaped structures. The dashed lines show the predictions of energies that the structures should have. In conditions where alkenes react rapidly, Benzene does not react. Besides, the electronic configuration of Benzene contributes to the explanation of its stability because, as are presented three pi bonds in the structure with six electrons, these fill the three bonding MOs of the benzene system [13].

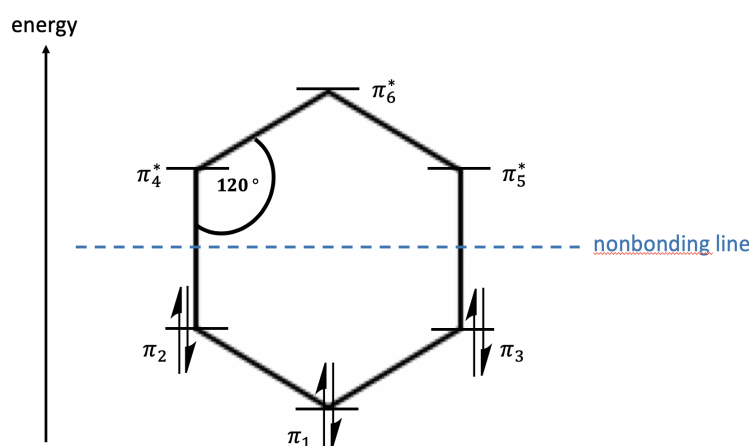


Figure 1.4: Energy diagram of the molecular orbital of Benzene.

Benzene has all bond angles of 120° . Since all the carbons in the structure have a hybridization sp^2 , each atom has a p orbital perpendicular to the plane of the ring. Simple bonds have a value of 1.47\AA and the double bonds 1.33\AA [13].

The fact that there is no exact solution to the Schrodinger equation to describe the chemical bond is necessary to specify some approximations. These approaches are based on two models: Valence Bond Theory (VBT) and Molecular Orbital Theory (MOT). In both theories, the orbitals' overlap is of utmost importance since the interaction between two atoms depends on the direction of the overlap.

While VBT explains that an optimal bond consists of the maximum overlap of two orbitals of the participating atoms, the MOT describes the bond as the overlapping of atomic orbitals that form molecular orbitals (bonding and anti-bonding molecular orbital) [14].

1.3 Slater-Koster terms overlaps and chemical bonds.

Over the years, the definition of the chemical bond has undergone several changes due to new epistemological foundations that occurred at different times, so that as new theories were developed, this concept was evolving [15]. The first theory of the chemical bond was developed by Gilbert Lewis, who defined the chemical bond as a pair of electrons shared by two atoms in such a way that the two fill their last shell, the valence shell [14]. Classically, the concept of the chemical bond, although a little coarse, is understood by the phenomenon by which atoms are kept paired by the presence of forces thus forming stable molecules. [14]. With the arrival of quantum mechanics, this concept evolved severely since it offers a fundamental description of nature at small scales. It explains that the chemical bond is the product of the overlapping of molecular orbitals of two atoms at a certain distance and energy.

To represent the chemical bond in terms of his energy and distances, we can use the tight-binding method that takes account that the electrons in a structure are strongly

located, such that the orbital overlap can be represented as a linear combination of the wave functions that describe the orbitals in an appropriated base. If we consider two atoms and we suppose that each atom has the atomic orbitals $\phi_{l,m} = |l, m\rangle$, identified by their angular momentum $l = s, p, d, \dots$ and by the quantum number m , and they are located on the positions \mathbf{R} and \mathbf{R}' , the overlap can be represented in the form:

$$V_{ll'm} \delta_{mm'} = \langle l', m', \mathbf{R}' | \hat{H} | l, m, \mathbf{R} \rangle, \quad (1.1)$$

where \hat{H} is the Hamiltonian for the energy of the bond, and the $V_{ll'}$ parameters are called Slater-Koster parameters if the relative vector $\mathbf{R} - \mathbf{R}'$ is parallel to the quantization axis of the orbitals ϕ_{lm} [5], [16], [17].

Each magnetic quantum number value is associated with a chemical bond type given by the overlapping of the atomic wave functions, and the different bond types have a specific m value, where $m=0$ represents bond type σ . The bond π has a value of $m=1$ and the bond type δ as a value $m=2$. The number of parameters is determined by the combination of the two orbitals and by the type of the chemical bond formed, as can be seen in figure 1.5.

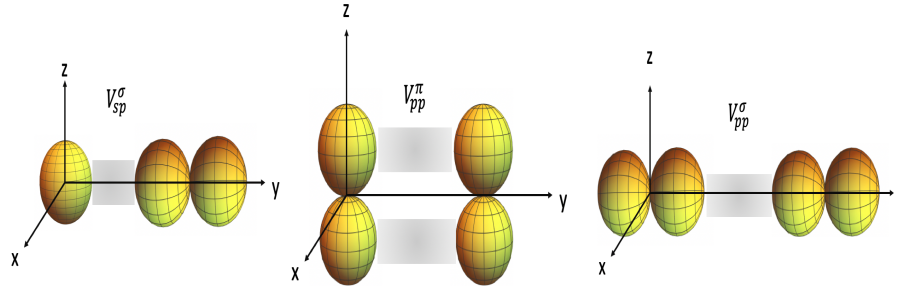


Figure 1.5: Diagram of the Slater-Koster parameters that represent the different types of σ and π bonds.

1.4 Atomic interactions

1.4.1 Spin-Orbit interaction

The spin-orbit interaction or spin-orbit coupling is a relativistic coupling between the angular momentum of a particle that moves in a potential and the spin of the particle. This relativistic effect is starting from the assumption that the nucleus surrounds the electron where the magnetic moment of the spin and the orbital angular momentum \mathbf{L} interact, and this creates a magnetic field \mathbf{B} [18],[19] (see figure 1.6). Knowing that each electron has an intrinsic property (electron spin) that induces a spin angular momentum, it creates the spin magnetic dipole moment (μ_s) and thus will be like a torque due \mathbf{B} .

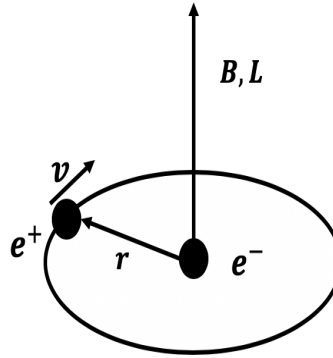


Figure 1.6: Spin-orbit interaction scheme.

$$\Delta E = -\mu_s \cdot \mathbf{B} \quad (1.2)$$

This magnetic field interacts with the electron magnetic moment (μ_e), so it produces interaction energy:

$$H_{so} = -\mu_s \cdot \mathbf{B}. \quad (1.3)$$

In the no-relativistic limit, the SO coupling appears as an additional term in the Schrodinger equation in the form

$$\hat{H}_{SO} = \frac{e\hbar}{4m_o^2c^2} \mathbf{s} \cdot (\mathbf{p} \times \Delta V), \quad (1.4)$$

where m_o and e are the mass and charge of the bare electron, c is the light velocity, \mathbf{p} is the linear momentum of the electron, V is the electrical potential and $\mathbf{s} = (\hbar/2)\sigma$ is the spin operator with σ the Pauli matrices[20]. In the approximation where the potential is spherically symmetric, the SO interaction operator for the movement of a particle with spin 1/2 is:

$$\hat{H}_{SO} = \lambda \mathbf{L} \cdot \mathbf{S} \quad (1.5)$$

where λ represent the atomic constant of SO coupling[20].

Element	meV
C	6[9]
N	-
Fe	
Ni	80[21]

Table 1.1: Spin-Orbit coupling values.

1.4.1.1 SO coupling between orbitals

Before calculating the SO coupling values, it is necessary to find an appropriate basis set in order to obtain the Spin-Orbit elements in the Hamiltonian. Starting from the equation (1.5) where \mathbf{L} and \mathbf{S} as variables, it can be denoted that both the angular momentum and the angular momentum of the spin do not commute [22]. In the case of \mathbf{L} its operators,

$[L_x, L_y]$ do not commute:

$$\begin{aligned} [L_x, L_y] &= [yp_z - zp_y, zp_x - xp_z] \\ &= [yp_z, zp_x] - [yp_z, xp_z] - [zp_x, zp_x] + [zp_y, xp_z] \\ &= i\hbar L_z. \end{aligned}$$

Thus, the full commutators for the angular momentum components are:

$$[L_x, L_y] = i\hbar L_z; \quad [L_x, L_z] = i\hbar L_y; \quad [L_y, L_z] = i\hbar L_x.$$

Then L_x, L_y and L_z are incompatible observables. But, if the angular momentum is squared, they commutes: [\[22\]](#)

$$[L^2, L] = 0$$

Now, the eigenvectors of L^2 and L_z satisfy:

$$\begin{aligned} L_{\pm} |l, m\rangle &= \hbar\sqrt{l(l+1) - m(m \pm 1)} |l, m \pm 1\rangle \\ L_z |l, m\rangle &= \hbar m |l, m\rangle \end{aligned}$$

Same for the angular momentum of spin, its fundamental commutation relations do not commute:

$$[S_x, S_y] = i\hbar S_z; \quad [S_x, S_z] = i\hbar S_y; \quad [S_y, S_z] = i\hbar S_x$$

The eigenvectors of S^2 and S_z satisfy:

$$\begin{aligned} S_{\pm} |s, m_s\rangle &= \hbar\sqrt{s(s+1) - m_s(m_s \pm 1)} |s, m_s \pm 1\rangle, \\ S_z |s, m_s\rangle &= \hbar m_s |s, m_s\rangle. \end{aligned}$$

The Hamiltonian rewriting in function of the \mathbf{L} and \mathbf{S} operators results:

$$H_{so} = \frac{\lambda}{2} [L_+ S_- + L_- S_+ + 2L_z S_z]. \quad (1.6)$$

As benzene has sp^2 , it presents p-type orbitals perpendicular to the plane of the ring, so for one carbon atom in the structure, these orbitals can be represented as [5]

$$\begin{aligned} |p_x\rangle &= -\frac{1}{\sqrt{2}}(|1, 1\rangle - |1, -1\rangle), \\ |p_y\rangle &= \frac{i}{\sqrt{2}}(|1, 1\rangle + |1, -1\rangle), \\ |p_z\rangle &= |1, 0\rangle. \end{aligned} \tag{1.7}$$

Once defined the appropriated basis set for the Spin-Orbit Hamiltonian, the coupling elements can be calculated. As an illustration, one of the calculation is shown below:

$$\begin{aligned} &\langle P_x, 1/2 | \hat{H}_{so} | P_z, 1/2 \rangle \\ &= \langle P_x, 1/2 | \frac{\lambda}{2} [L_+ S_- + L_- S_+ + 2L_z S_z] | P_z, 1/2 \rangle \\ &= \langle P_x, 1/2 | \frac{\lambda}{2} [L_+ S_- |1, 0, 1/2\rangle + L_- S_+ |1, 0, 1/2\rangle + 2L_z S_z |1, 0, 1/2\rangle] \\ &= \langle P_x, 1/2 | \frac{\lambda}{2} \hbar^2 \sqrt{2} |1, 1, 1/2\rangle \\ &= \frac{1}{\sqrt{2}} (\langle 1, 1, 1/2 | - \langle 1, -1, 1/2 |) \frac{\lambda}{2} \hbar^2 \sqrt{2} |1, 1, 1/2\rangle \\ &= \langle 1, 1, 1/2 | \frac{\lambda}{2} \hbar^2 |1, 1, 1/2\rangle - \langle 1, -1, 1/2 | \frac{\lambda}{2} \hbar^2 |1, 1, 1/2\rangle \\ &= \lambda \hbar^2 \end{aligned}$$

Performing the calculations for all possible combinations of orbitals and reducing in the spin-space, we obtain:

	$ p_x\rangle$	$ p_y\rangle$	$ p_z\rangle$
$\langle p_x $	0	$-i\frac{\lambda}{2}s_z$	$i\frac{\lambda}{2}s_y$
$\langle p_y $	$i\frac{\lambda}{2}s_z$	0	$-\frac{\lambda}{2}is_x$
$\langle p_z $	$-i\frac{\lambda}{2}s_y$	$i\frac{\lambda}{2}s_x$	0

Table 1.2: Expected Spin-Orbit values that connect the atomic orbitals.

where s_x , s_y and s_z are the spin matrices, which in turn can be written according to the Pauli matrix σ_x , σ_y and σ_z . The relationship between the spin matrices and the Pauli matrices are the next:

$$\hat{S}_i = \frac{\hbar}{2}\sigma_i \quad (1.8)$$

1.4.2 Stark effect

Analogue of the Zeeman effect, the Stark effect originates from the interaction between the dipole moments of diatomic molecules and an external electric field. Described for the first time by Johannes Stark in 1913, this effect explains the displacement and separation of rotational or rovibrational spectral lines due to a static electric field E along the z-axis. [23]. The Stark effect is described as

$$\hat{H}_S = -eE_z\hat{z}, \quad (1.9)$$

where e is the charge of the electron and \hat{z} is the unit vector along the z-axis where the only nonzero element for this coupling is [5]:

$$\langle p_z | H_S | s \rangle = 2ea_0E_z = \xi sp. \quad (1.10)$$

There are two types of Stark effect, while the first order Stark effect that depends linearly on the intensity of the electric field the second order Stark effect has a quadratic dependence on the intensity of the electric field [23].

1.5 Computational Methodology

Avogadro is a visualization and molecular edition program oriented to computational chemistry, molecular modeling, and more [24]. Among its tools, it presents Orca extensions where it is possible to develop geometric optimization of the created molecules. Orca, meanwhile, is a package of quantum chemistry programs with a variety of electronic structure methods such as Density Function Theory (DFT), semi-empiric methods, among others [25]. Orca can optimize molecular geometries and estimate specific quantum parameters at different levels of theory. Besides the methods mentioned above, high-level ab-initio quantum chemical methods are included to increase precision degree. [24]

The Orca program allows creating inputs with specific methods that users use to perform the best matches of the created molecule and the process. The program is based on calculations of first principles, which means that it assumes only basic and well-established laws, excluding simplified models and external parameters. The conjectures are based on wave functions to reach the final results.

The program can use methods and adequate basis-set for proper optimization. The methods and basis-set used for the computational analysis are listed below:

- def2- is a basis-set used to represent the electronic wave function. def2-SVP (Spin Valence Polarization) was used to take account of the polarization functions on all atoms, including hydrogen atoms.
- B3LYP is a class of approximation of the functional of exchange and correlation in the Density Functional Theory (DFT) used to optimize the molecular geometries [25]. It is built by three parameters (Hartree–Fock method + Local Density Approximation + General Gradient Approximations) so that it more closely approximates the functional exchange and correlation to the wave function of the study system.
- D3BJ is the dispersion correction of DFT calculations required for any geometric calculations because the interaction energy is much better. Also, intermolecular

interaction can be treated.

CHAPTER 2

COMPUTATIONAL ANALYSIS OF THE MOLECULAR STRUCTURE: HELICENE

In this section, it is shown a computational procedure that allows obtaining specific values to characterize the molecular structure by physical parameters such as atomic distances. In this case, Avogadro program is used for the design of the Helicene molecule (taken as a model molecule) and Orca for the orbitals calculations. This procedure was done to verify if exists any difference in the helical pitch and the band-gap energies of the Helicene enantiomers' structure.

Two inputs were generated for each Helicene structure with a certain number of benzene rings. One of them was made with a dispersion arrangement and the other, without that arrangement. This process was carried out to compare the calculations of the p orbitals of the Helicene.

The method used for the calculations was a hybrid method of the functional density theory (B3LYP) with a direct optimization in the input and not in the Avogadro program. This method is used due its reproduced quite accurately all kind of properties of molecular systems thanks, among other qualities, to the 20% of the Hartree-Fock method introduced. To describe the density distribution of the molecule, as well as molecular orbitals of Helicene, a basis-set was used. In this case, a Split Valence Polarization (SVP) basis-set due

to its calculation speed.

Finally, the dispersion correction used in one of the inputs has the purpose of calculating weak intermolecular interactions of aromatic π compounds that are not taken into account and that change the energy of the orbitals.

Once these considerations are placed in the input shown in figures [2.1](#) and [2.2](#):

```
# avogadro generated ORCA input file
# Basic Mode
#
! B3LYP D3BJ OPT def2-SVP

* xyz 0 1
C      -4.68406      3.57579      0.82732
C      -5.31963      2.39400      0.40971
C      -3.26768      3.62845      1.01051
C      -2.54719      2.47870      0.60177
C      -4.57300      1.26482      0.09822
```

Figure 2.1: Input with Dispersion Correction.

```
# avogadro generated ORCA input file
# Basic Mode
#
! B3LYP OPT def2-SVP

* xyz 0 1
C      -4.68406      3.57579      0.82732
C      -5.31963      2.39400      0.40971
C      -3.26768      3.62845      1.01051
C      -2.54719      2.47870      0.60177
C      -4.57300      1.26482      0.09822
```

Figure 2.2: Input with No Dispersion Correction.

To see the orbitals p, the next code is inserted:

```
*
%output
Print [ P_Basis ] 2
Print [ P_MOs ] 1
end
```

Figure 2.3: Code to show p-orbitals.

With these processes, were calculated Helicene Band-gap of different lengths and the distance of reference Carbon atoms.

Once Orca has finished, the results are loaded in Avogadro to show p-orbitals and the Band-gap energies:

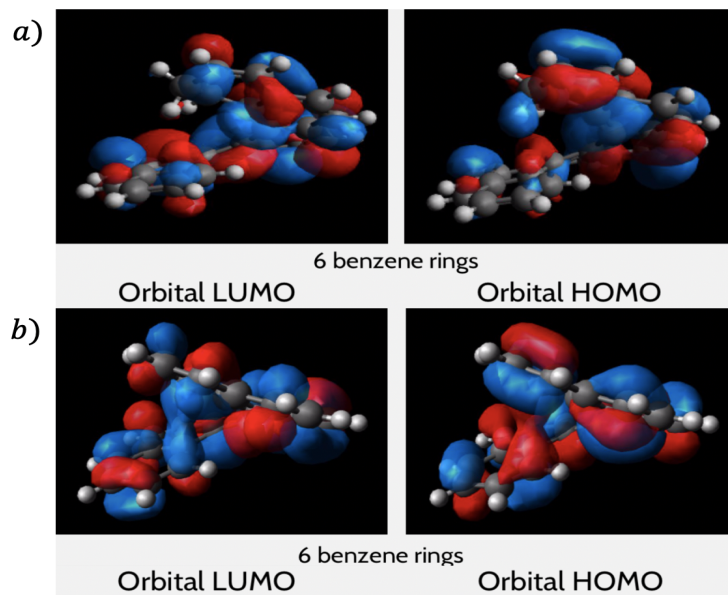


Figure 2.4: 6 Benzene Rings-Helicene with: a) correction dispersion and b) no correction dispersion.

In the table [2.1](#) is shown the respective energies of each type of Helicene's structures:

Cycles Number	DC*	Homo (eV)	Lumo (eV)	Bandgap (eV)
5	Yes	-5.654	-1.501	4.153
	No	-5.651	-1.503	4.148
6	Yes	-5.591	-1.672	3.919
	No	-5.355	-1.612	3.743
7	Yes	-5.508	-1.714	3.794
	No	-5.524	-1.701	3.823
12	No	-4.948	-2.102	2.846

Table 2.1: Results-Structure 1. (Fig 1.1 (a))

Cycles Number	DC*	Homo (eV)	Lumo (eV)	Bandgap (eV)
5	Yes	-5.653	-1.501	4.152
	No	-5.650	-1.503	4.147
6	Yes	-5.591	-1.672	3.919
	No	-5.593	-1.676	3.917
7	Yes	-5.508	-1.712	3.796
	No	-5.522	-1.697	3.825
12	No	-4.945	-2.1	2.845

Table 2.2: Results-Structure 2. (Fig 1.1 (b))

Through the computational analysis, was obtained the helical pitch for Helicene of 6 rings of benzene, the structure 1 of the Helicene has a value of 3.377Å, while the structure 2, its helical pitch is 3.173Å (Figure 1.1). Shen and his collaborator found that experimentally the helical pitch of Helicene is 3, 20Å [12].

Table 2.1 and Table 2.2 also show the bandgap energies of the two helicene structures with a different number of benzenes with the presence and absence of dispersion correction (DC^*). Even though the band gap values for the same benzene cycles number of the same structure are different, the values are quite the same for the same cycle number when dispersion correction is present. Hence, it does not matter what Helicene structure is used to carry out a theoretical experiment as long as dispersion correction is included.

CHAPTER 3

ANALYTICAL SLATER-KOSTER ELEMENTS

In this section, it is shown the calculation of the SK elements that describe the overlaps of atomic orbitals of two neighboring atoms in a molecule. As a model molecule is considered the benzene, which is the basic unit that makes up the Helicene.

The molecule is parameterized in a specific coordinate system such that SK elements are a function of the atomic distances and the angles between the vectors that connect the atoms. The variation of these quantities allows testing the behavior of the SK elements under molecular deformations, which can be induced mechanically or with radiation to produce vibrations, etc.

3.1 Slater-Koster (SK) elements in general coordinate systems

3.1.1 SK elements with $\{s, p_x, p_y\}$ in the xy -plane and p_z orthogonal.

To obtain the Slater-Koster (SK) elements, is taken account that each atom can be modeled with a set of orbitals $\{s, p_x, p_y, p_z\}$ where p_x and p_y orbitals are contained in the plane

and the p_z orbitals are oriented perpendicular to the plane (see Fig. 3.1). Due to the symmetry of benzene, the relative vector $\mathbf{R}' - \mathbf{R}$ is not parallel to the axis of quantization of the orbitals, so that the overlapping of orbitals is not only given by the SK elements in their conventional form, $V_{\mu\mu'}$, but in general, they are represented as a linear combination of these.

According to Ando [26], the SK overlaps in this general case, for two neighboring atoms (on sites denoted by i and j) is given by

$$E_{\mu\mu'}^{ij} = (\hat{n}(\mu_i)^\parallel \cdot \hat{n}(\mu_j)^\parallel) V_{\mu\mu'}^\sigma + (\hat{n}(\mu_i)^\perp \cdot \hat{n}(\mu_j)^\perp) V_{\mu\mu'}^\pi, \quad (3.1)$$

where $V_{\mu\mu'}^{\sigma,\pi}$ are Slater-Koster overlaps, $\hat{n}(\mu_i)$ is the unit vector in the direction of μ orbital in the site i , $\hat{n}(\mu_i)^\parallel$ is the projection of $\hat{n}(\mu_i)$ in the direction of \mathbf{R}_{ji} and $\hat{n}(\mu_i)^\perp$ is the projection in the perpendicular direction, such that:

$$\hat{n}(\mu_i)^\parallel = \frac{(\mathbf{R}_{ji}, \hat{n}(\mu_i))}{\mathbf{R}_{ji}, \mathbf{R}_{ji}} \mathbf{R}_{ji}, \quad (3.2)$$

$$\hat{n}(\mu_i)^\perp = \hat{n}(\mu_i) - \frac{(\mathbf{R}_{ji}, \hat{n}(\mu_i))}{\mathbf{R}_{ji}, \mathbf{R}_{ji}} \mathbf{R}_{ji}. \quad (3.3)$$

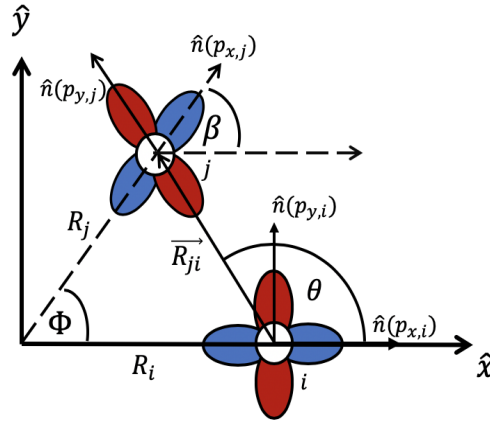


Figure 3.1: Scheme showing two orbitals located in R_i and R_j positions, and the unit vectors that indicate the direction of the atomic orbitals.

Equation (3.1) can be rewritten as:

$$E_{\mu\mu'}^{ij} = \langle \mu_i | V | \mu_j' \rangle = (\hat{n}(\mu_i), \hat{n}(\mu_j')) V_{\mu\mu'}^\pi + \frac{(\mathbf{R}_{\mathbf{j}i}, \hat{n}(\mu_i))(\mathbf{R}_{\mathbf{j}i}, \hat{n}(\mu_j'))}{\mathbf{R}_{\mathbf{j}i}, \mathbf{R}_{\mathbf{j}i}} (V_{\mu\mu'}^\sigma - V_{\mu\mu'}^\pi). \quad (3.4)$$

Considering the physical variables shown in figure 3.1 and using equation (3.4) we obtained the SK expressions of all possible overlaps between the orbitals:

$$\begin{aligned} E_{sx}^{ij} &= V_{sx}^\pi - V_{sx}^\pi \cos(\beta - \theta) + V_{sx}^\sigma \cos(\beta - \theta) = E_{xs}^j \\ E_{sy}^{ij} &= V_{sy}^\pi - V_{sy}^\pi \sin(\beta - \theta) + V_{sy}^\sigma \sin(\beta - \theta) = E_{ys}^j \\ E_{sz}^{ij} &= 0 = E_{zs}^j \\ E_{xx}^{ij} &= (\cos \beta - \cos(\beta - \theta) \cos \theta) V_{xx}^\pi + \cos(\beta - \theta) \cos \theta V_{xx}^\sigma = E_{xx}^j \\ E_{xy}^{ij} &= (-\sin \beta + \cos \theta \sin(\beta - \theta)) V_{xy}^\pi - \cos \theta \sin(\beta - \theta) V_{xy}^\sigma = E_{yx}^j \\ E_{xz}^{ij} &= 0 = E_{zx}^j \\ E_{yy}^{ij} &= (\cos \beta + \sin(\beta - \theta) \sin \theta) V_{yy}^\pi - \sin(\beta - \theta) \sin \theta V_{yy}^\sigma = E_{yy}^j \\ E_{yz}^{ij} &= 0 = E_{zy}^j \\ E_{zz}^{ij} &= V_{zz}^\pi = E_{zz}^j \\ E_{xs}^{ij} &= V_{sx}^\pi + \cos \theta (V_{sx}^\sigma - V_{sx}^\pi) = E_{sx}^j \\ E_{ys}^{ij} &= V_{sy}^\pi + \sin \theta (V_{sy}^\sigma - V_{sy}^\pi) = E_{sy}^j \\ E_{zs}^{ij} &= 0 = E_{sz}^j \\ E_{yx}^{ij} &= (\sin \beta - \sin \theta \cos(\beta - \theta)) V_{pp}^\pi + \sin \theta \cos(\beta - \theta) V_{pp}^\sigma = E_{xy}^j \\ E_{zx}^{ij} &= 0 = E_{xz}^j \\ E_{zy}^{ij} &= 0 = E_{yz}^j \end{aligned}$$

Table 3.1: Slater-Koster overlaps between orbitals on sites i and j .

The Slater-Koster matrix elements $V_{ll'}$ obey the rule: $V_{ll'} = (-1)^{l+l'} V_{l'l}$ where l and l' are the atomic angular momentum.

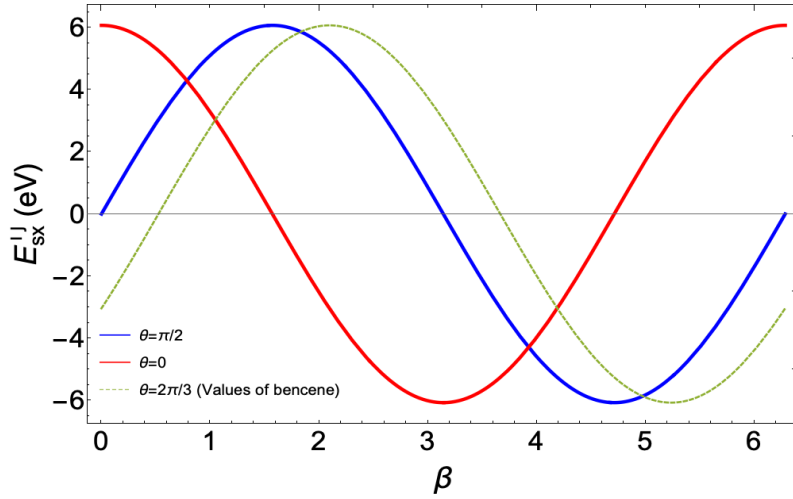


Figure 3.2: The SK overlap E_{sx} as a function of β for different values of θ . To calculate the values of $V_{\mu\mu'}$ the used distance between atoms is $\mathbf{R} = 1.42 \text{ \AA}$.

In Figure [3.2](#), it is shown the behavior of the E_{sx} element for different values of the parameters, when β changes, the relative angle between the s and p_x orbitals (see FIG. [3.1](#)). When $\theta = 0$ and $\beta = 0$, s and p_x orbitals form a sigma bond, and the value shown corresponds to the maximum value of the bond, it is to say $E_{sx} = V_{sp}$. As beta grows, the magnitude of the σ bond decreases because there will only be a partial overlap between the orbitals, and, when $\theta = \pi/2$ and $\beta = 0$ the bond dies because the p_x orbital is orthogonal with s orbital. The negative sign of the coupling corresponds to the orientation of the z orbital by which the sigma bond is formed.

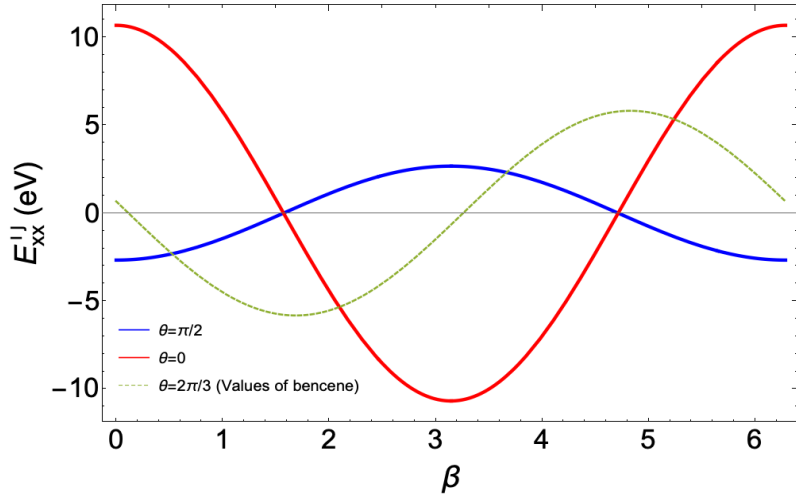


Figure 3.3: The SK overlap E_{xx} as a function of β for different values of θ . To calculate the values of $V_{\mu\mu'}$ the used distance between atoms is $\mathbf{R} = 1.42\text{\AA}$, $K_{pp}^{\sigma} = -0.81$ and $K_{pp}^{\pi} = 3.24$.

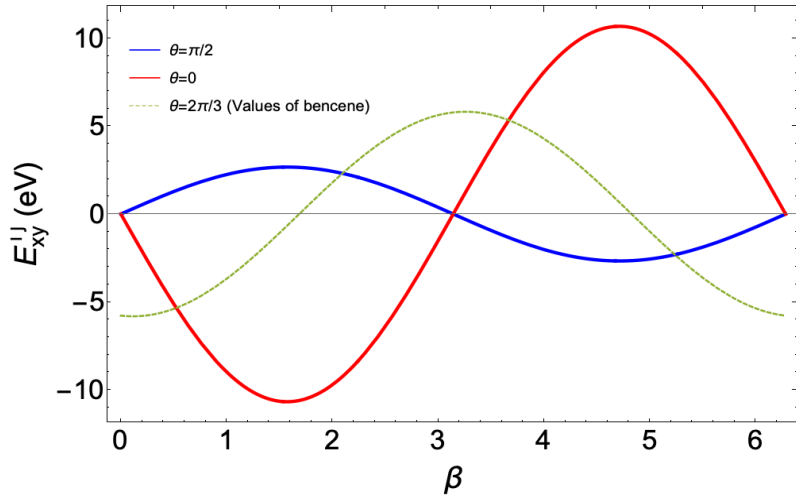


Figure 3.4: The SK overlap E_{xy} as a function of β for different values of θ . To calculate the values of $V_{\mu\mu'}$ the used distance between atoms is $\mathbf{R} = 1.42\text{\AA}$, $K_{pp}^{\sigma} = -0.81$ and $K_{pp}^{\pi} = 3.24$.

Analogously, the E_{xx} and E_{xy} are shown in figures [3.3](#) and [3.4](#), respectively. In Fig. [3.3](#) it is possible to see that when $\beta = 0$, and $\theta = 0$, overlap between p_x orbitals is maximum,

and correspond a σ -bond equal to the corresponding V_{pp} overlap. In Fig 3.4, for $\theta = 0$ and $\theta = \pi/2$, when $\beta = 0$ the overlaps are zero, because p_x and p_y are orthogonal. The other values correspond to the overlaps that have a partial contribution of σ and π couplings. It also shows how this bond would vary for characteristic Benzene values if any deformation in the structure of the molecule is made.

As β changes, the coupling between the two orbitals varies where the maximums are σ couplings and the minimum π -type couplings.

3.1.2 SK elements with $\{s, p_x, p_y\}$ in the xy -plane and p_z with a component in the z -axis.

In the previous section, the Slater-Koster elements have been made for a specific orbitals' orientation where three angles are taking account (See Figure 3.1).

A new scheme is presented below (Figure 3.5), to find general overlapping equations. In this case, it is consider a more general orientation and position of the orbitals than in the previous case. Depending on the molecule and the information associated with its parameters, one or the other can be used.

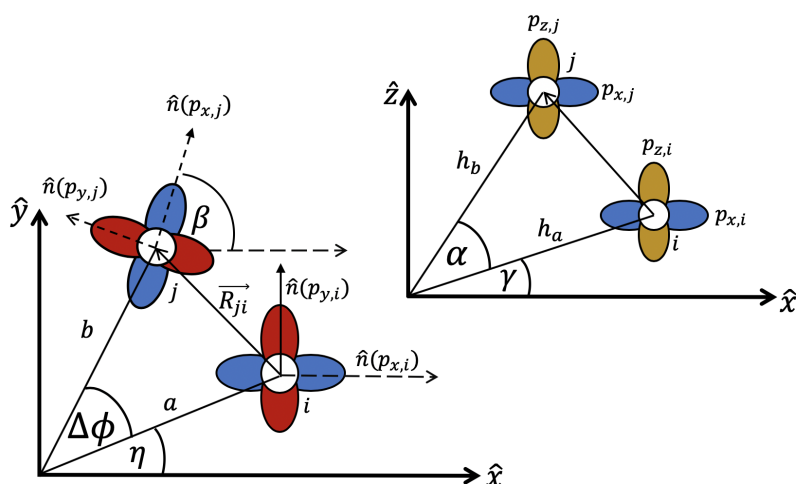


Figure 3.5: General scheme of orbitals overlap in a specific coordinate system. In this case, the p_z orbital has a component in the z -axis.

The directions for the orbitals in sites i and j in these conditions can be represented as follows:

$$\begin{aligned}\hat{n}(s_i)^\parallel &= \hat{R}_{j_i} \\ \hat{n}(x_i) &= \hat{x} \\ \hat{n}(y_i) &= \hat{y} \\ \hat{n}(z_i) &= \hat{z}\end{aligned}\tag{3.5}$$

$$\begin{aligned}\hat{n}(s_j)^\parallel &= \hat{R}_{j_j} \\ \hat{n}(x_j) &= \cos \beta \hat{x} + \sin \beta \hat{y} \\ \hat{n}(y_j) &= \cos (\beta + \pi/2) \hat{x} + \sin (\beta + \pi/2) \hat{y} \\ \hat{n}(z_j) &= \hat{z},\end{aligned}\tag{3.6}$$

and the distance between i and j atom is

$$|\mathbf{R}_{j_i}| = (b \cos (\Delta\phi + \eta) - a \cos \eta) \hat{x} + (b \sin (\Delta\phi + \eta) - a \sin \eta) \hat{y} + (h_b \sin (\alpha + \gamma) - h_a \sin \gamma) \hat{z}\tag{3.7}$$

where $\Delta\phi$ is the angle between the vectors a and b that represent the positions of two atoms in the lattice.

Using this values, the SK overlaps obtained are shown in table [3.2](#)

$$\begin{aligned}
 E_{sx}^{vj} &= \frac{(b \cos(\beta - \Delta\phi - \eta) - a \cos(\beta - \eta))}{R_{j_1}} V_{sx}^\sigma = E_{xs}^j \\
 E_{sy}^{vj} &= \frac{(-b \sin(\beta - \Delta\phi - \eta) + a \sin(\beta - \eta))}{R_{j_1}} V_{sy}^\sigma = E_{ys}^j \\
 E_{sz}^{vj} &= \frac{(h_b \sin(\alpha + \gamma) - h_a \sin \gamma)}{R_{j_1}} V_{sz}^\sigma = E_{zs}^j \\
 E_{xx}^{vj} &= \cos \beta V_{xx}^\pi - \frac{(b \cos(\beta - \Delta\phi - \eta) - a \cos(\beta - \eta))(b \cos(\Delta\phi - \eta) - a \cos \eta)}{R_{j_1}^2} (V_{xx}^\pi - V_{xx}^\sigma) = E_{xx}^j \\
 E_{xy}^{vj} &= -\sin \beta V_{xy}^\pi + \frac{(b \cos(\Delta\phi - \eta) - a \cos \eta)(b \sin(\beta - \Delta\phi - \eta) - a \sin(\beta - \eta))}{R_{j_1}^2} (V_{xy}^\pi - V_{xy}^\sigma) = E_{xy}^j \\
 E_{xz}^{vj} &= \frac{(b \cos(\Delta\phi + \eta) - a \cos \eta)(h_b \sin(\alpha + \gamma) - h_a \sin \gamma)}{R_{j_1}} (V_{yz}^\sigma - V_{yz}^\pi) = E_{zx}^j \\
 E_{yy}^{vj} &= \cos \beta V_{yy}^\pi + \frac{(b \sin(\beta - \Delta\phi - \eta) - a \sin(\beta - \eta))(b \sin(\Delta\phi - \eta) - a \sin \eta)}{R_{j_1}^2} (V_{yy}^\pi - V_{yy}^\sigma) = E_{yy}^j \\
 E_{yz}^{vj} &= \frac{(b \sin(\Delta\phi + \eta) - a \sin \eta)(h_b \sin(\alpha + \gamma) - h_a \sin \gamma)}{R_{j_1}} (V_{yz}^\sigma - V_{yz}^\pi) = E_{zy}^j \\
 E_{zz}^{vj} &= V_{zz}^\pi + \frac{(h_b \sin(\alpha + \gamma) - h_a \sin \gamma)(h_b \sin(\alpha + \gamma) - h_a \sin \gamma)}{R_{j_1}} (V_{yy}^\sigma - V_{yy}^\pi) = E_{zz}^j \\
 E_{xs}^{vj} &= \frac{(b \cos(\Delta\phi - \eta) - a \cos \eta)}{R_{j_1}} V_{sx}^\sigma = E_{sx}^j \\
 E_{ys}^{vj} &= \frac{(b \sin(\Delta\phi - \eta) - a \sin \eta)}{R_{j_1}} V_{sy}^\sigma = E_{sy}^j \\
 E_{zs}^{vj} &= \frac{(h_b \sin(\alpha + \gamma) - h_a \sin \gamma)}{R_{j_1}} V_{sz}^\sigma = E_{sz}^j \\
 E_{yx}^{vj} &= \sin \beta V_{xy}^\pi - \frac{(b \cos(\beta - \Delta\phi - \eta) - a \cos(\beta - \eta))(b \sin(\Delta\phi - \eta) - a \sin \eta)}{R_{j_1}^2} (V_{xy}^\pi - V_{xy}^\sigma) = E_{xy}^j \\
 E_{zx}^{vj} &= -\frac{(a \cos(\beta - \eta) - b \cos(\beta - \Delta\phi - \eta))(h_a \sin \gamma - h_b \sin(\alpha + \gamma))}{R_{j_1}^2} (V_{zx}^\pi - V_{zx}^\sigma) = E_{xz}^j \\
 E_{zy}^{vj} &= \frac{(a \sin(\beta - \eta) - b \sin(\beta - \Delta\phi - \eta))(h_a \sin \gamma - h_b \sin(\alpha + \gamma))}{R_{j_1}^2} (V_{zy}^\pi - V_{zy}^\sigma) = E_{yz}^j
 \end{aligned}$$

Table 3.2: General Overlapping Equations

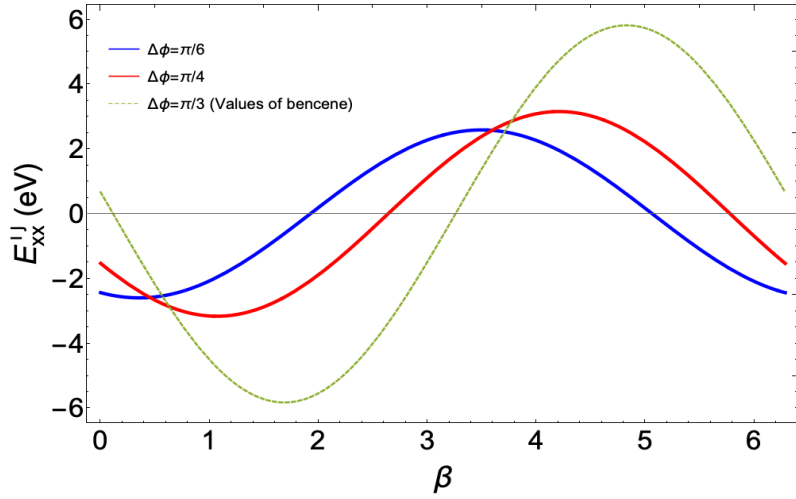


Figure 3.6: The SK overlap E_{xx} as a function of β for different values of θ . To calculate the values of $V_{\mu\mu'}$ the used distance between atoms is $\mathbf{R} = 1.42\text{\AA}$, $K_{pp}^{\sigma} = -0.81$ and $K_{pp}^{\pi} = 3.24$.

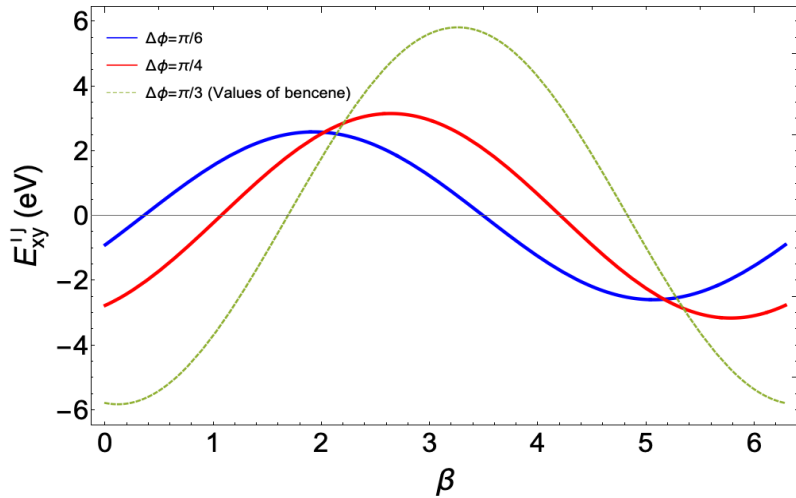


Figure 3.7: The SK overlap E_{xy} as a function of β for different values of θ . To calculate the values of $V_{\mu\mu'}$ the used distance between atoms is $\mathbf{R} = 1.42\text{\AA}$, $K_{pp}^{\sigma} = -0.81$ and $K_{pp}^{\pi} = 3.24$.

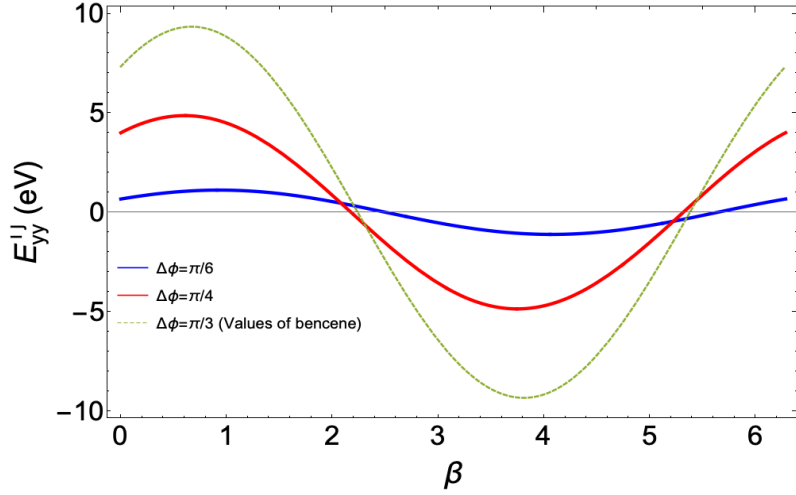


Figure 3.8: The SK overlap E_{yy}^{II} as a function of β for different values of θ . To calculate the values of $V_{\mu\mu'}$ the used distance between atoms is $\mathbf{R} = 1.42\text{\AA}$, $K_{pp}^{\sigma} = -0.81$ and $K_{pp}^{\pi} = 3.24$.

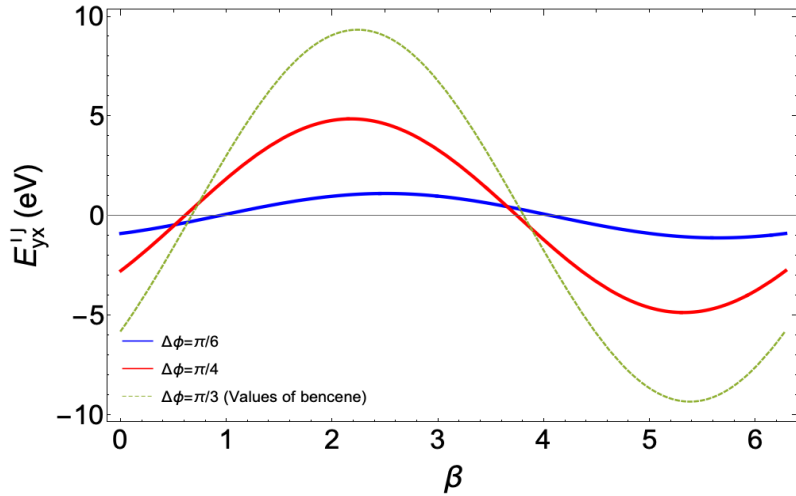


Figure 3.9: The SK overlap E_{yx}^{II} as a function of β for different values of θ . To calculate the values of $V_{\mu\mu'}$ the used distance between atoms is $\mathbf{R} = 1.42\text{\AA}$, $K_{pp}^{\sigma} = -0.81$ and $K_{pp}^{\pi} = 3.24$.

The interpretation of the graphics obtained is analogous to the previous section. When

the overlaps are equal to zero, it means that the orbitals are orthogonal and for values where the module is maximum, there are pure π or σ overlaps between the orbitals.

3.1.3 Verification of the Slater-Koster expressions

In this section, the expressions obtained in the previous subsections are used in order to reproduce the results reported in molecules: DNA and nanotubes.

3.1.3.1 DNA model in 2D projection

Equations from Table [3.1](#) have been tested in DNA model to prove their validity. The first test was done according to Varela et al. research [\[20\]](#) in which the effective spin-orbit couplings in an analytical tight-binding model of DNA were carried out. Considering the parameters of the model presented in Varela research (see Figure [3.10](#)), the parameters for the equations of Figure [3.1](#), were adapted to DNA model such that $\Phi = \beta = \Delta\phi$ and $R_i = R_j = a$. For the overlaps in DNA, $R_n = 2a$, $\Delta\phi = \pi$ and $b = 0$. Of course, in this case we consider only the projection in the xy plane of the equations (the pitch of the helix is not considered, therefore $b = 0$ is used in the model)

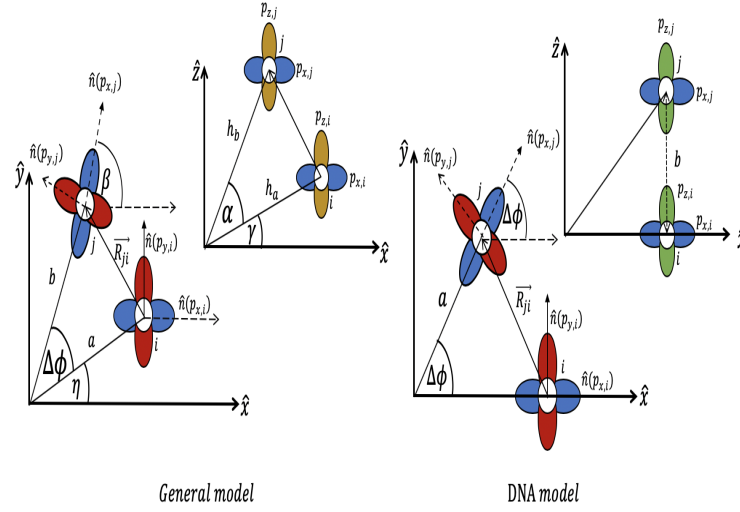


Figure 3.10: DNA molecular structure model in a XY plane [20]. For the equations shown, we used just to the verification that $b = 0$.

These values were inserted into the equations resulting in the same value reported in the paper:

$$\begin{aligned}
 E_{sx}^{vj} &= -V_{sx}^{\sigma}, & E_{sy}^{vj} &= 0, & E_{sz}^{vj} &= 0, \\
 E_{xx}^{vj} &= -V_{xx}^{\sigma}, & E_{yy}^{vj} &= -V_{yy}^{\pi}, & E_{zz}^{vj} &= V_{zz}^{\pi}, \\
 E_{xy}^{vj} &= 0, & E_{xz}^{vj} &= 0, & E_{yz}^{vj} &= 0 \quad [20].
 \end{aligned}$$

3.1.3.2 Nanotubes in a 3D model

In this case, are used the equations [3.2] to compute the SK terms for a model of nanotube proposed by Ando [26].

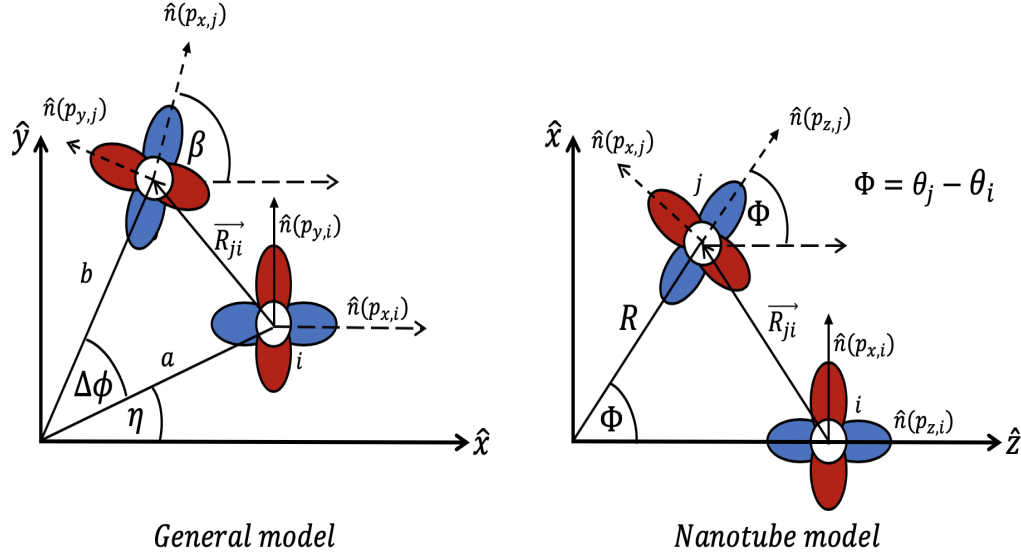


Figure 3.11: The our general scheme and the Nanotube model scheme that show the orientations of the orbitals.

To adapt the general model to Nanotube overlapping scheme (Figure [3.12](#)), The following equivalences between the parameters have been used:

$$\eta = 0, \quad \beta = \Phi, \quad \Phi = \theta_j - \theta_i, \quad a = b = R, \quad |R_{ji}|^2 = (1/3)a^2,$$

$$\hat{x} \rightarrow \hat{z}, \quad \hat{y} \rightarrow \hat{x}, \quad \hat{z} \rightarrow \hat{y}$$

Notice that in this case, it is needed to do a rotation of the coordinate system, because orbitals p_z in nanotubes are in the radial direction. The orbital orientation of atom j is:

$$\hat{n}(z_j) = \hat{z},$$

$$\hat{n}(x_j) = \cos(\Phi + \pi/2)\hat{z} + \sin(\Phi + \pi/2)\hat{x},$$

$$\hat{n}(y_j) = Y_{jn},$$

$$\mathbf{R}_{jn} = R[(\cos \Phi - 1)\hat{z} + \sin \Phi \hat{x}].$$

Now, using our expression shown in [3.2](#) are proved with Nanotube parameters, for example, for E_{zx}^{vj} element:

$$E_{zx}^{vj} = \sin(\theta_i - \theta_j)V_{pp}^\pi + (V_{pp}^\sigma - V_{pp}^\pi)\frac{3R^2}{a^2}(1 - \cos(\theta_i - \theta_j))(\sin(\theta_i - \theta_j))$$

3.1.3.3 DNA in a 3D model

Equations [3.2](#) are used to compute the SK terms for a model of DNA general, such that the pitch $b \neq 0$.

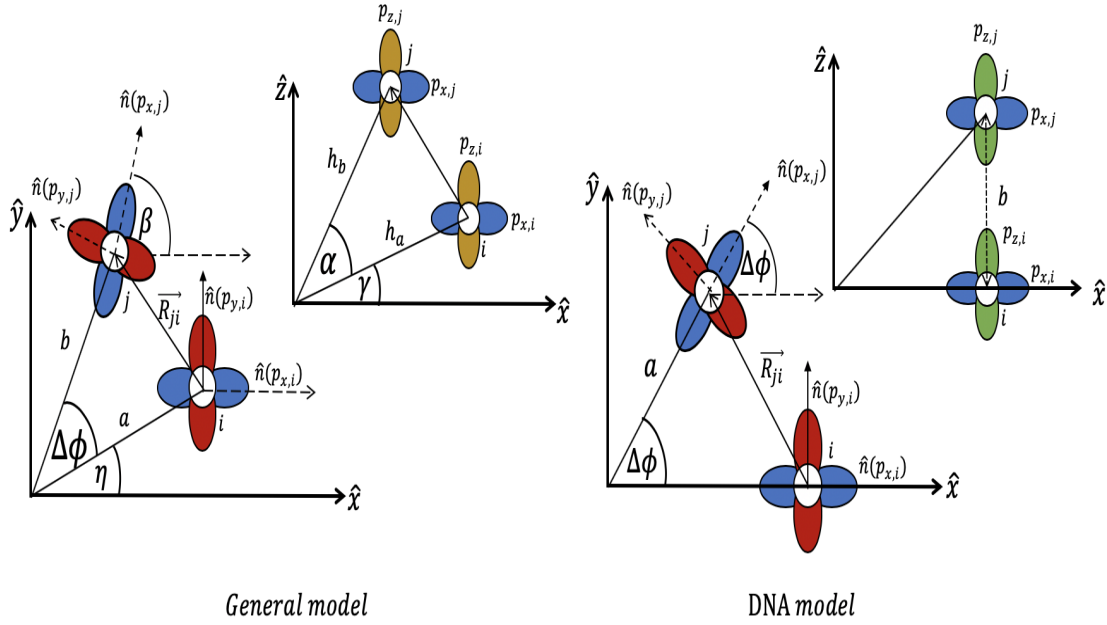


Figure 3.12: General and the DNA model schemes that show the orientations of the orbitals. In the DNA model, b is the pitch of the molecule and a is the radius of the helix.

The next relations are considered to adapt the general model to DNA overlapping scheme:

$$\eta = 0, \quad \beta = \Delta\phi, \quad b = a$$

and the orbital orientations of atom j are:

$$\begin{aligned}\hat{n}(s_j) &= \hat{R}_{jz} \\ \hat{n}(x_j) &= \cos \phi \hat{x} + \sin \phi \hat{y} \\ \hat{n}(y_j) &= \cos(\phi + \pi/2) \hat{x} + \sin(\phi + \pi/2) \hat{y} \\ |R_{jn}|^2 &= 4a^2 \sin^2\left(\frac{\Delta\phi}{2}\right)\end{aligned}$$

Now, equations of Table [3.2](#) are proved with DNA parameters:

$$E_{sx}^{vj} = \frac{a(1 - \cos \Delta\phi)}{|R_{jn}|} V_{sp}^\sigma$$

$$E_{sy}^{vj} = \frac{a \sin(\phi_j - \phi_i)}{|R_{jn}|} V_{sp}^\sigma$$

$$E_{sz}^{vj} = \frac{b(\phi_j - \phi_i)}{2\pi |R_{jn}|} V_{sp}^\sigma$$

$$E_{xx}^{vj} = \frac{\cos \Delta\phi |R_{jn}|^2 V_{pp}^\pi - (V_{pp}^\sigma - V_{pp}^\pi) 4a^2 \sin^4\left(\frac{\Delta\phi}{2}\right)}{|R_{jn}|^2}$$

$$E_{yy}^{vj} = \frac{\cos \Delta\phi |R_{jn}|^2 V_{pp}^\pi + a^2 \sin^2 \Delta\phi (V_{pp}^\sigma - V_{pp}^\pi)}{|R_{jn}|^2}$$

$$E_{xy}^{vj} = \frac{(|R_{jn}|^2 V_{pp}^\pi + (V_{pp}^\sigma - V_{pp}^\pi) 2a^2 \sin^2\left(\frac{\Delta\phi}{2}\right)) (\sin \phi_i - \phi_j)}{|R_{jn}|^2}$$

$$E_{xz}^{ij} = \frac{2ab \sin^2\left(\frac{\Delta\phi}{2}\right)(\phi_i - \phi_j)(V_{pp}^\sigma - V_{pp}^\pi)}{2\pi|R_{jn}|^2}$$

$$E_{yz}^{ij} = \frac{ab \sin(\phi_j - \phi_i)(\phi_j - \phi_i)(V_{pp}^\sigma - V_{pp}^\pi)}{2\pi|R_{jn}|^2}$$

3.2 Use of the SK model with a molecule example: Benzene

3.2.1 Benzene parameterization

The position vector for each benzene carbon in the coordination system \hat{X} , \hat{Y} , \hat{Z} (Figure 3.13) is labeled as \mathbf{R}_i , where i is the number of atoms such that $i = 1, \dots, 6$. in counterclockwise. a is designated as the radius of benzene and $\Delta\phi$ is the angle between two consecutive atoms. The position vectors \mathbf{R}_i in term of this parameters, in a 2D coordinate system of Fig. 3.13, are written as:

$$\mathbf{R}_i = a \cos[(i-1)\Delta\phi]\hat{X} + a \sin[(i-1)\Delta\phi]\hat{Y}, \quad (3.8)$$

and, the vector that represents the distance between two consecutive carbon atoms is labeled \mathbf{R}_j and given by the equation:

$$\mathbf{R}_j = \mathbf{R}_j - \mathbf{R}_i = (a \cos(j-1)\Delta\phi - a \cos(i-1)\Delta\phi)\hat{X} + (a \sin(j-1)\Delta\phi - a \sin(i-1)\Delta\phi)\hat{Y} \quad (3.9)$$

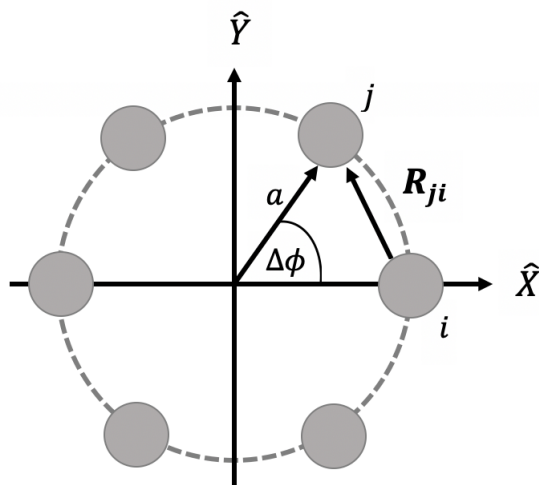


Figure 3.13: Benzene carbons in the X-Y plane where $\Delta\phi$ is the angle between consecutive carbons and \mathbf{R}_{ji} is the distance between two atoms.

3.2.2 The SK elements and the dependence with deformations in the benzene model

For the two schemes (Figure 3.1 and Figure 3.5) and set of equations (Table 3.1 and Table 3.2), the results of benzene orbital overlapping in function of β are presented in the graphics 3.14. This figure 3.14 shows only the coupling of the p_x orbitals of atoms i and j as the β advances, keeping θ constant at a value of $\theta = 2\pi/3$. When $\beta = 0$, there is coupling with a combination of sigma and pi interactions due to the orbitals p_x are not parallel. Throughout the 360 degrees, the orbitals of the atom j will rotate, maintaining a combination of sigma and pi interactions in their coupling as can be seen in points a, b and c. In a and c , the point has reached the minimum and maximum points, respectively. In them, there is no single π or σ coupling but a combination of these two couplings with different proportions. While at point a , there is a higher π coupling, at point c , the σ coupling overlaps predominates. On the other hand, at point b , there is no coupling because when $\beta = 3.25642$, the orbitals p_{x_i} and p_{x_j} they are orthogonal between them. The point value that represent benzene overlap is c .

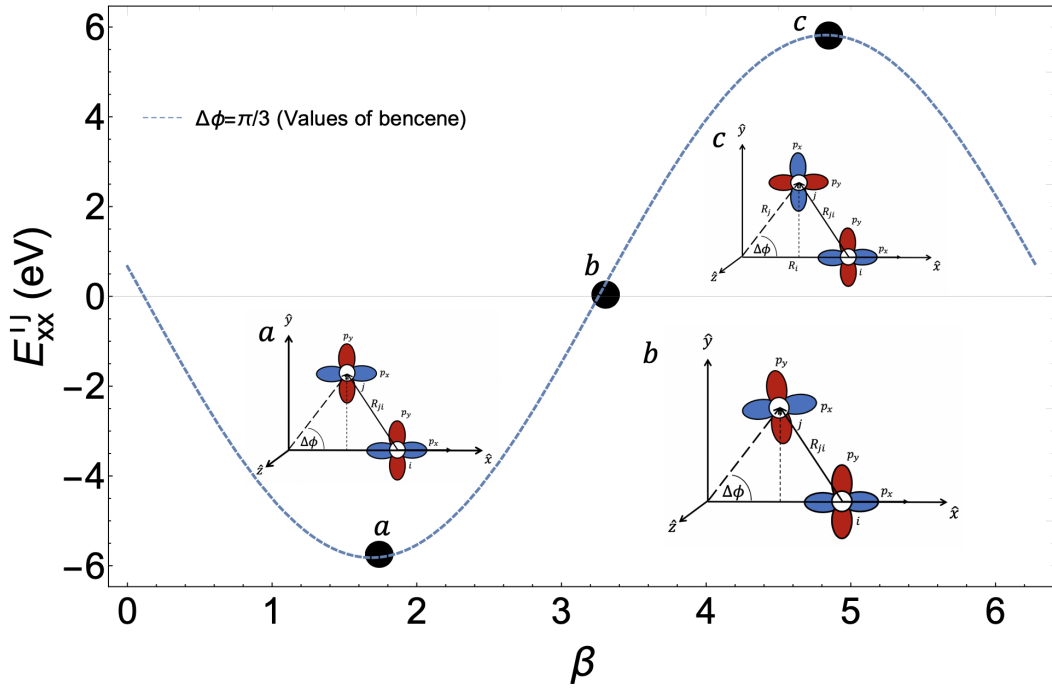


Figure 3.14: Representation of benzene's two p_x -orbitals coupling.

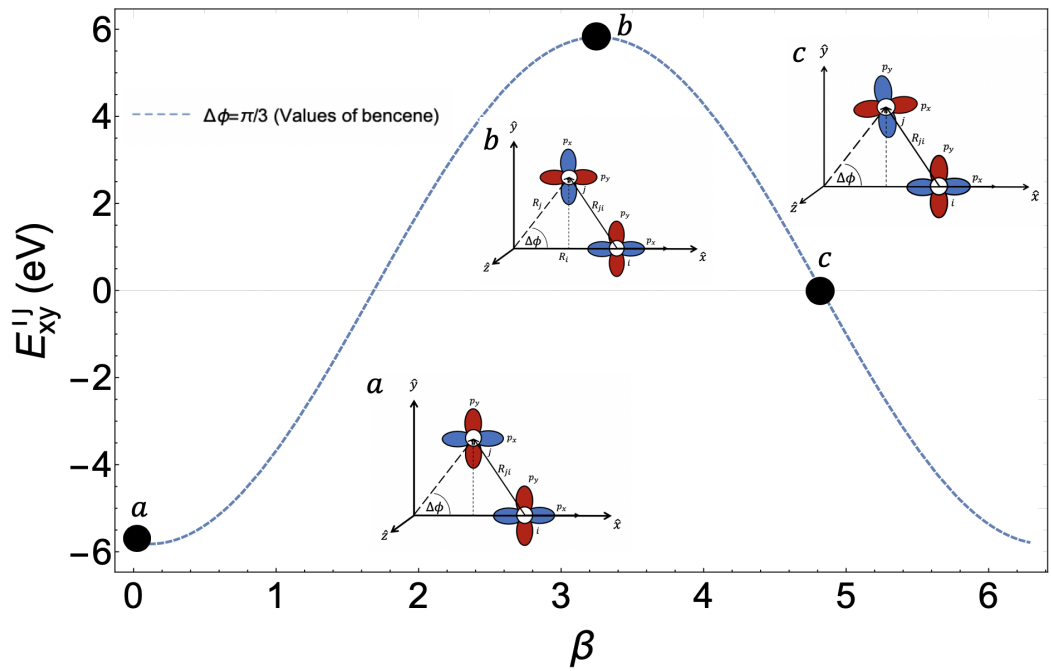


Figure 3.15: Representation of benzene's p_x^2 and p_y^2 orbitals coupling.

Figure 3.15 shows the $p_x^i-p_y^j$ orbital coupling that begins at the minimum point with a combination of pi and sigma bonds where pi predominates, at $\beta = 0$. At $\beta = \pi$, the bond stands out is sigma. Finally, at $\beta = 276.57^\circ$, there is no coupling due to the orthogonal position of the orbitals.

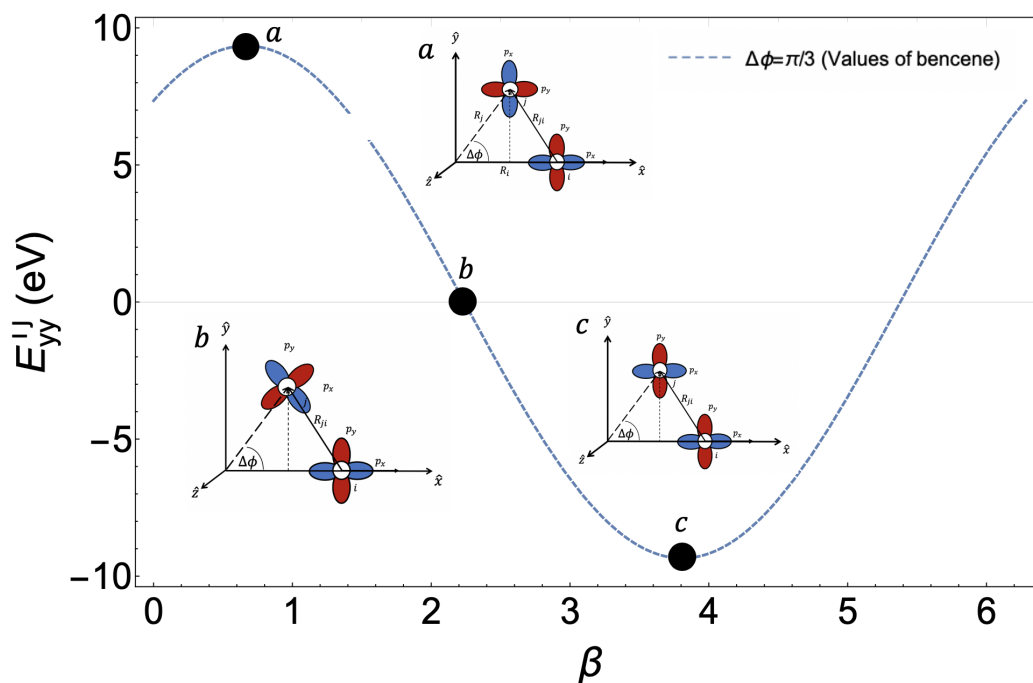


Figure 3.16: Representation of benzene's two p_y orbitals coupling.

The graphics shown are the same regardless of the schemes used. This is also a verification of the expressions in the different coordinate systems shown, so the equations are equivalent. As the beta angle begins to rotate, three main points are distinguished, the minimum and maximum where the pi and sigma bonds predominate, respectively, and the point where it cuts the x-axis at which there is no interaction because the orbitals are orthogonal between them. Sigma and pi values are not fully achieved because the orbitals are not parallel.

3.3 Chapter conclusions

The deformations shown can be induced by several mechanisms. For example, by mechanical deformations produced by stretching of the molecule, means of external electric fields or radiation that produce vibrations of the structure, etc. Of course, the deformations shown in the graphs are a function of all the possible values that the relative orientations between the orbitals can take. However, these modifications, experimentally, will be restricted by the actual bonds associated with the molecules and the ability of the molecules to be deformed without breaking.

As some theoretical models show, these overlaps can be proportionally related to the interactions present in the Hamiltonians that describe the molecules. Understanding the behavior of these elements can help maximize other properties of organic molecules, for example, the ability to conduct a specific spin current.

CHAPTER 4

PATHS THAT CONNECT P_Z ORBITALS THROUGH INTERACTIONS AND THE SLATER-KOSTER TERMS

One methods to determine tight-binding Hamiltonian, involves considering Feynman type-diagrams that effectively connect the orbitals at two neighboring sites in the molecular structure. These paths contribute to the Hamiltonian only when the present interactions connect the atomic orbitals effectively, such that

$$H = H_K + H_S + H_{ISO} + H_R + \dots, \quad (4.1)$$

where the term H_K take account the contribution only associated with the Slater-Koster elements, or kinetic terms; the second term in the Hamiltonian, H_S is the contribution of pure Stark effect (ξ_{sp}); the third term, H_{ISO} corresponds to the intrinsic spin-orbit (ξ_p) coupling contribution; the H_R is a Rashba contribution that results from the coupling between orbitals by the ISO and Stark interactions; etc.

In this section we have derived all the possible paths that result from considering the SO interaction ξ_p and the Stark effect ξ_{sp} , with the corresponding kinetic term and the SK overlaps of the orbitals to first and second order. Here is presented one case where one electron located in p_z orbital of atom i and goes to p_z orbital of atom j .

$p_z^i \xleftrightarrow{E_{zz}^{ij}} p_z^j$
$p_z^i \xleftrightarrow{\xi_{sp}} s^i \xleftrightarrow{E_{sz}^{ij}} p_z^j$
$p_z^i \xleftrightarrow{\xi_p} p_x^i \xleftrightarrow{E_{xz}^{ij}} p_z^j$
$p_z^i \xleftrightarrow{\xi_p} p_y^i \xleftrightarrow{E_{yz}^{ij}} p_z^j$
$p_z^i \xleftrightarrow{\xi_{sp}} s^i \xleftrightarrow{E_{sx}^{ij}} p_x^j \xleftrightarrow{\xi_p} p_z^j$
$p_z^i \xleftrightarrow{\xi_{sp}} s^i \xleftrightarrow{E_{sy}^{ij}} p_y^j \xleftrightarrow{\xi_p} p_z^j$
$p_z^i \xleftrightarrow{E_{zs}^{ij}} s^j \xleftrightarrow{\xi_{sp}} p_x^j \xleftrightarrow{\xi_p} p_z^j$
$p_z^i \xleftrightarrow{E_{zs}^{ij}} s^j \xleftrightarrow{\xi_{sp}} p_y^j \xleftrightarrow{\xi_p} p_z^j$

Table 4.1: First order's possible paths from p_z^i to p_z^j .

The paths that connect p_z -orbitals are shown in table [4.1](#), to the first order in the interactions. The arrow in the two directions takes into account that for each path indicated to the right, there is a path associated with the conjugate complex, which ensures the hermiticity of the terms. When there are no presence of external interactions such as the external electric field, only kinetic energy can move one electron from atom i to atom j :

$$p_z^i \xleftrightarrow{E_{zz}^{ij}} p_z^j$$

When there is an electric field in the direction of the z-axis, the electron can move from p_z^i to the orbital s^i and finally through kinetic energy it reaches to p_z^j .

$$p_z^i \xleftrightarrow{\xi_{sp}} s^i \xleftrightarrow{E_{sz}^{ij}} p_z^j$$

Now, when there is an interaction between the magnetic moment of the electron spin and the angular momentum of the electron orbital, an effective magnetic field is created where it can go from the p_z orbital to the other p orbitals of the same atom and thus together with kinetic energy, the electron reaches the atom j .

$$p_z^i \xleftrightarrow{\xi_p} p_x^i \xleftrightarrow{E_{xz}^{ij}} p_z^j$$

$$p_z^i \xleftrightarrow{\xi_p} p_y^i \xleftrightarrow{E_{yz}^{ij}} p_z^j$$

When there is the presence of an external electric field, effective magnetic field and kinetic energy, the possible paths that the electron can take are the following:

$$p_z^i \xleftrightarrow{\xi_{sp}} s^i \xleftrightarrow{E_{sx}^{ij}} p_x^j \xleftrightarrow{\xi_p} p_z^j$$

$$p_z^i \xleftrightarrow{\xi_{sp}} s^i \xleftrightarrow{E_{sy}^{ij}} p_y^j \xleftrightarrow{\xi_p} p_z^j$$

$$p_z^i \xleftrightarrow{E_{zs}^{ij}} s^j \xleftrightarrow{\xi_{sp}} p_x^j \xleftrightarrow{\xi_p} p_z^j$$

$$p_z^i \xleftrightarrow{E_{zs}^{ij}} s^j \xleftrightarrow{\xi_{sp}} p_y^j \xleftrightarrow{\xi_p} p_z^j$$

When interactions can be repeated twice, the possible electron transport paths are:

$p_z^i \xleftrightarrow{\xi_p} p_x^i \xleftrightarrow{E_{xx}^{ij}} p_x^j \xleftrightarrow{\xi_p} p_z^j$
$p_z^i \xleftrightarrow{\xi_p} p_x^i \xleftrightarrow{E_{xy}^{ij}} p_y^j \xleftrightarrow{\xi_p} p_z^j$
$p_z^i \xleftrightarrow{\xi_p} p_y^i \xleftrightarrow{E_{yy}^{ij}} p_y^j \xleftrightarrow{\xi_p} p_z^j$
$p_z^i \xleftrightarrow{\xi_{sp}} s^i \xleftrightarrow{E_{ss}^{ij}} s^j \xleftrightarrow{\xi_{sp}} p_z^j$
$p_z^i \xleftrightarrow{\xi_p} p_x^i \xleftrightarrow{\xi_{sp}} s^i \xleftrightarrow{E_{sx}^{ij}} p_x^j \xleftrightarrow{\xi_p} p_z^j$
$p_z^i \xleftrightarrow{\xi_p} p_y^i \xleftrightarrow{\xi_{sp}} s^i \xleftrightarrow{E_{sy}^{ij}} p_y^j \xleftrightarrow{\xi_p} p_z^j$
$p_z^i \xleftrightarrow{\xi_p} p_y^i \xleftrightarrow{\xi_{sp}} s^i \xleftrightarrow{E_{sy}^{ij}} p_y^j \xleftrightarrow{\xi_p} p_z^j$
$p_z^i \xleftrightarrow{\xi_{sp}} s^i \xleftrightarrow{\xi_{sp}} p_x^i \xleftrightarrow{E_{xx}^{ij}} p_x^j \xleftrightarrow{\xi_p} p_z^j$
$p_z^i \xleftrightarrow{\xi_{sp}} s^i \xleftrightarrow{\xi_{sp}} p_x^i \xleftrightarrow{E_{xy}^{ij}} p_y^j \xleftrightarrow{\xi_p} p_z^j$
$p_z^i \xleftrightarrow{\xi_{sp}} s^i \xleftrightarrow{\xi_{sp}} p_y^i \xleftrightarrow{E_{yx}^{ij}} p_x^j \xleftrightarrow{\xi_p} p_z^j$
$p_z^i \xleftrightarrow{\xi_{sp}} s^i \xleftrightarrow{\xi_{sp}} p_y^i \xleftrightarrow{E_{yy}^{ij}} p_y^j \xleftrightarrow{\xi_p} p_z^j$
$p_z^i \xleftrightarrow{\xi_p} p_x^i \xleftrightarrow{\xi_p} p_y^i \xleftrightarrow{E_{yx}^{ij}} p_x^j \xleftrightarrow{\xi_{sp}} s^j \xleftrightarrow{\xi_{sp}} p_z^j$
$p_z^i \xleftrightarrow{\xi_p} p_x^i \xleftrightarrow{\xi_p} p_y^i \xleftrightarrow{E_{yy}^{ij}} p_y^j \xleftrightarrow{\xi_{sp}} s^j \xleftrightarrow{\xi_{sp}} p_z^j$
$p_z^i \xleftrightarrow{\xi_p} p_y^i \xleftrightarrow{\xi_p} p_x^i \xleftrightarrow{E_{xx}^{ij}} p_x^j \xleftrightarrow{\xi_{sp}} s^j \xleftrightarrow{\xi_{sp}} p_z^j$
$p_z^i \xleftrightarrow{\xi_p} p_y^i \xleftrightarrow{\xi_p} p_x^i \xleftrightarrow{E_{xy}^{ij}} p_y^j \xleftrightarrow{\xi_{sp}} s^j \xleftrightarrow{\xi_{sp}} p_z^j$

Table 4.2: Second order's possible paths from p_z^i to p_z^j .

For the case of the second order's possible paths, when kinetic energy and Spin-Orbit interaction ξ_p is activated, the possible paths are:

$$\begin{aligned}
 p_z^i &\xleftrightarrow{\xi_p} p_x^i \xleftrightarrow{E_{xx}^{ij}} p_x^j \xleftrightarrow{\xi_p} p_z^j \\
 p_z^i &\xleftrightarrow{\xi_p} p_x^i \xleftrightarrow{E_{xy}^{ij}} p_y^j \xleftrightarrow{\xi_p} p_z^j \\
 p_z^i &\xleftrightarrow{\xi_p} p_y^i \xleftrightarrow{E_{yy}^{ij}} p_y^j \xleftrightarrow{\xi_p} p_z^j
 \end{aligned}$$

On the other hand, when kinetic energy and an electric field is applied, the only available pathway is:

$$p_z^i \xleftrightarrow{\xi_{sp}} s^i \xleftrightarrow{E_{ss}^{ij}} s^j \xleftrightarrow{\xi_{sp}} p_z^j$$

Combining kinetic energy, SO and Stark interactions twice, the potential paths are founded in Table [4.2](#).

4.1 Chapter conclusions

The possible paths electrons can take in electron transportation at first and second order are examined when different interactions are activated. When some of the interactions contribute to a first-order term in the Hamiltonian, these are usually those of the greatest contribution by which higher-order ones can be neglected, if a perturbative method is consider. In addition, the presence of a specific interaction does not necessarily ensure that it generates a term in the Hamiltonian since this will depend on the geometry of the system that influences the value of the terms SK. An example is the case of graphene, where despite considering intrinsic interaction SO, as the structure is flat, the first-order contribution dies because the SK overlaps are zero, and the largest contribution of the SO interaction is second order in the disturbance. However, if any graphene deformation is induced, for example, to generate nanotubes, the deformation couples the orbitals so that a first-order term is achieved. Therefore, for a complete description of effective Hamiltonians, interactions and geometry must be taken into account.

CONCLUSIONS

We have derived expressions in specific coordinate systems and with characteristic parameters of the molecules, from orbital overlaps that are a representation of the chemical bonds formed by atoms, the Slater-Koster elements. For this, a computational analysis of a specific molecular structure was carried out, and after the determination of the SK elements, all possible paths that contribute to the effective Hamiltonian interactions that the molecule describes are determined.

Through computational analysis, it was demonstrated that bandgap energy is independent of Helicene model molecule turns as long as the dispersion correction is applied because this correction considers weak intermolecular interactions of pi-aromatic compounds. This computational analysis can be used to model molecular structures and obtain values of characteristic parameters to be used in the subsequent calculation of overlaps.

The study of the atomic-orbital coupling using Slater-Koster type elements was done in function of the physical parameters of the molecular structure. These elements generally correspond to a chemical bond resulting from the partial overlapping of the pi and sigma orbitals between the atoms. Understanding the behavior of these overlaps with variations

in the parameters allows identifying the way in which a structure can be physically deformed in order to maximize the contribution to a specific bond, allowing deformations to generate an increase in the interactions associated with the effective Hamiltonian. It is important to indicate that the actual deformations that can be made to a molecular structure are restricted by the mechanical properties of the molecules, such as Young's module.

Finally, the different paths connecting the p_z orbitals of two atoms are written, in the presence of overlaps and SO and Stark interactions. On these paths, it is explicit that changing the molecule with deformations changes the SK overlaps and therefore changes the contributions of the interactions in the effective Hamiltonians, increasing the probability of the affected paths. Therefore, the expressions derived in combination with the behavior of the atomic orbitals (or chemical bonds) are a guide for studying the general behavior of the terms that appear in the Hamiltonian tight-binding effective, and therefore of the total energy associated with the molecule.

BIBLIOGRAPHY

- [1] B. Göhler et al Science **331**, 894 (2011).
- [2] Oligopeptides M. Kettner, B. Göhler, H. Zacharias, D. Mishra, V. Kiran, R. Naaman, C. Fontanesi, David H. Waldeck, Sławomir Sęk, Jan Pawłowski, and Joanna Juhaniewicz. Spinfiltering in electron transport through chiral oligopeptides. The Journal of Physical Chemistry C, 119(26):14542–14547, 2015. bibitem Gutierrez R. Gutierrez; E. Diaz; R. Naaman and G. Cuniberti. Spin-selective transport through helical molecular systems. Phys. Rev. B, **85**, 2012.
- [3] R. Naaman and D. H. Waldeck. Chiral-induced spin selectivity effect. Phys. Chem. Lett., **3 (16)**, 2012.
- [4] William Thomson and Baron Kelvin. Baltimore Lectures on Molecular Dynamics and the Wave Theory of Light. 2010.
- [5] S. Varela. Transporte y polarización electrónica a través de películas quirales. 2016.
- [6] K. I. Shinohara; Y. Sannohe; S. Kaieda; K. I. Tanaka; H. Osuga; H. Tahara; Y. Xu; T. Kawase; T. Bando and H. Sugiyama. A chiral wedge molecule inhibits telomerase activity. J. Am. Chem. Soc., 2010.

- [7] S. Yeganeh; M. A. Ratner; E. Medina and V. Mujica. *J. Chem. Phys.*, **131**, 2009.
- [8] T. R. Pan; A. M. Guo and Q. F. Sun. Spin-polarized electron transport through helicene molecular junctions. *Phys. Rev. B*, **235448**, 2016.
- [9] Solmar Varela Salazar, Vladimiro Mujica, and Ernesto Medina. Spin-orbit coupling-modulation in dna by mechanical deformations. *CHIMIA International Journal for Chemistry*, 72(6):411–417, 2018.
- [10] S Varela, B Montañes, F López, B Berche, B Guillot, V Mujica, and E Medina. Intrinsic rashba coupling due to hydrogen bonding in dna. *The Journal of Chemical Physics*, 151(12):125102, 2019.
- [11] Ken Kamikawa. Recent development of helicene synthesis. *Journal of Synthetic Organic Chemistry, Japan*, 72(1):58–67, 2014.
- [12] Yun Shen and Chuan-Feng Chen. Helicenes: Synthesis and applications. *Chemical Reviews*, 112(3):1463–1535, 2012. PMID: 22017405.
- [13] L. G. Wade. *Organic Chemistry*, Pearson, 2013.
- [14] O. Lombardi; J. Camilo and M. Gonzalez. Entre mecánica cuántica y estructuras químicas: ¿a qué refiere la química cuántica? 2012.
- [15] M. E. González-Felipe. El enlace químico en la educación secundaria. estrategias didácticas que permiten superar las dificultades de aprendizaje. **270**, 2017.
- [16] J. C. Slater and G. F. Koster. Simplified lcao method for the periodic potential problem. *Phys. Rev.*, 94:1498–1524, Jun 1954.
- [17] Sergej Konschuh, Martin Gmitra, and Jaroslav Fabian. Tight-binding theory of the spin-orbit coupling in graphene. *Phys. Rev. B*, 82:245412, Dec 2010.
- [18] José Miguel Lia. Interacción espín-órbita en anillos cuánticos semiconductores delgados.

- [19] Alastair I. M. Rae. *Quantum Mechanics*, Fourth edition. 2002.
- [20] Solmar Varela, Vladimiro Mujica, and Ernesto Medina. Effective spin-orbit couplings in an analytical tight-binding model of dna: Spin filtering and chiral spin transport. *Phys. Rev. B*, 93:155436, Apr 2016.
- [21] J. Bünemann, F. Gebhard, T. Ohm, S. Weiser, and W. Weber. Spin-orbit coupling in ferromagnetic nickel. *Phys. Rev. Lett.*, 101:236404, Dec 2008.
- [22] David J. Griffiths. *Introduction to Quantum Mechanics (2nd Edition)*. Pearson Prentice Hall, 2nd edition, April 2004.
- [23] Michael Schmitt and Leo Meerts. Chapter 5 - structures and dipole moments of molecules in their electronically excited states. In Jaan Laane, editor, *Frontiers and Advances in Molecular Spectroscopy*, pages 143 – 193. Elsevier, 2018.
- [24] Marcus D. Hanwell, Donald Ephraim Curtis, David C. Lonie, Tim Vandermeersch, Eva Zurek, and Geoffrey R. Hutchison. Avogadro: an advanced semantic chemical editor, visualization, and analysis platform. In *Journal of Cheminformatics*, 2012.
- [25] Frank Neese. The orca program system. *Wiley Interdisciplinary Reviews: Computational Molecular Science*, 2(1):73–78, 2012.
- [26] Tsuneya Ando. Spin-orbit interaction in carbon nanotubes. *Journal of the Physical Society of Japan*, 69(6):1757–1763, 2000.